Biomedicine & Pharmacotherapy 141 (2021) 111861

Contents lists available at ScienceDirect

Biomedicine & Pharmacotherapy

journal homepage: www.elsevier.com/locate/biopha

Pharmacodynamic and pharmacokinetic profiles of a neurotensin receptor type 2 (NTS2) analgesic macrocyclic analog

Magali Chartier [a,1], Michael Desgagné [a,1], Marc Sousbie [a], Charles Rumsby [a], Lucie Chevillard [b], Léa Théroux [a], Lounès Haroune [a], Jérôme Côté [a], Jean-Michel Longpré [a], Pierre-Luc Boudreault [a], Éric Marsault [a,2], Philippe Sarret [a,*,2]

[a] Institut de Pharmacologie de Sherbrooke, Department of Pharmacology and Physiology, Faculty of Medicine and Health Sciences, Université de Sherbrooke, Sherbrooke, QC, Canada
[b] Inserm, UMR-S 1144, Université de Paris, Paris, France

ARTICLE INFO

Keywords:
Macrocycle
Metabolic stability
Analgesia
Pain
Opioid-sparing effects

ABSTRACT

The current opioid crisis highlights the urgent need to develop safe and effective pain medications. Thus, neurotensin (NT) compounds represent a promising approach, as the antinociceptive effects of NT are mediated by activation of the two G protein-coupled receptor subtypes (i.e., NTS1 and NTS2) and produce potent opioid-independent analgesia. Here, we describe the synthesis and pharmacodynamic and pharmacokinetic properties of the first constrained NTS2 macrocyclic NT(8–13) analog. The Tyr^{11} residue of NT(8–13) was replaced with a Trp residue to achieve NTS2 selectivity, and a rationally designed side-chain to side-chain macrocyclization reaction was applied between Lys^{8} and Trp^{11} to constrain the peptide in an active binding conformation and limit its recognition by proteolytic enzymes. The resulting macrocyclic peptide, CR-01-64, exhibited high-affinity for NTS2 (K_i 7.0 nM), with a more than 125-fold selectivity over NTS1, as well as an improved plasma stability profile ($t_{1/2} > 24$ h) compared with NT ($t_{1/2} \sim 2$ min). Following intrathecal administration, CR-01-64 exerted dose-dependent and long-lasting analgesic effects in acute ($ED_{50} = 4.6$ μg/kg) and tonic ($ED_{50} = 7.1$ μg/kg) pain models as well as strong mechanical anti-allodynic effects in the CFA-induced chronic inflammatory pain model. Of particular importance, this constrained NTS2 analog exerted potent nonopioid antinociceptive effects and potentiated opioid-induced analgesia when combined with morphine. At high doses, CR-01-64 did not cause hypothermia or ileum relaxation, although it did induce mild and short-term hypotension, all of which are physiological effects associated with NTS1 activation. Overall, these results demonstrate the strong therapeutic potential of NTS2-selective analogs for the management of pain.

1. Introduction

Chronic pain management represents a daily public health challenge, as 20% of the global population lives with different types of disabilities, including physical impairment and psychological distress [1]. Despite a better understanding of the underlying mechanisms of pain and the identification of novel pain targets [2], epidemiological studies still reveal that over 75% of patients with chronic pain taking prescribed analgesic medications are not satisfied with their current available treatment, mainly due to the development of debilitating side effects [3]. In light of the current opioid crisis, alternative options to conventional pain medications that exhibit high analgesic effectiveness, a low risk of adverse effects and no abuse liability are needed to adequately relieve chronic pain [2,4].

* Correspondence to: Department of Pharmacology-Physiology, Faculty of Medicine and Health Sciences, Université de Sherbrooke, 3001, 12e Avenue Nord, Sherbrooke, Québec, Canada J1H 5N4.

E-mail addresses: Magali.Chartier@USherbrooke.ca (M. Chartier), Michael.Desgagne@USherbrooke.ca (M. Desgagné), Marc.Sousbie@USherbrooke.ca (M. Sousbie), Charles.Rumsby@USherbrooke.ca (C. Rumsby), luciechevillard@gmail.com (L. Chevillard), Lea.Theroux@USherbrooke.ca (L. Théroux), Lounes.Haroune@USherbrooke.ca (L. Haroune), Jerome.Cote@USherbrooke.ca (J. Côté), Jean-Michel.Longpre@USherbrooke.ca (J.-M. Longpré), Pierre-Luc.Boudreault@USherbrooke.ca (P.-L. Boudreault), Philippe.Sarret@USherbrooke.ca (É. Marsault), philippe.sarret@usherbrooke.ca (P. Sarret).

[1] Authors contributed equally to this work.
[2] Authors contributed equally to directing this study.

https://doi.org/10.1016/j.biopha.2021.111861
Received 22 March 2021; Received in revised form 22 June 2021; Accepted 28 June 2021
Available online 3 July 2021

Neurotensin (NT) is an endogenous tridecapeptide (pGlu-Leu-Tyr-Glu-Asn-Lys-Pro-Arg-Arg-Pro-Tyr-Ile-Leu-OH) that functions as a neuromodulator/neurotransmitter in the central nervous system (CNS), modulating dopamine transmission, stimulating hypothalamic-pituitary-adrenal activity and exerting potent hypothermic and analgesic effects [5–11]. In the periphery, NT also behaves as a paracrine and endocrine hormone of the cardiovascular system and the digestive tract [12,13]. Regarding its analgesic action, NT was found to produce a potent opioid-independent antinociceptive response, since the administration of the opioid antagonists, naloxone or naltrexone is not effective in reversing NT-induced analgesia [14–22]. Importantly, compelling evidence also indicates that the analgesic potencies of NT and its analogs are superior to morphine at equimolar doses in various pain models [23–26].

NT exerts its antinociceptive action through the activation of two distinct G protein-coupled receptors (GPCRs), namely, NTS1 and NTS2 [8,9,27,28]. Both receptors and the NT peptide are highly abundant in the ascending and descending pain control pathways, particularly in the dorsal root ganglia, spinal cord dorsal horn, periaqueductal gray, raphe magnus and pallidus, and rostroventral medulla [28–37]. However, in contrast to NTS2, which is predominantly expressed in brain structures associated with pain modulation, NT binding to NTS1 also regulates blood pressure, myocardial contractility, core body temperature and gastrointestinal motility [12,13,38–40]. Consequently, the NTS2 receptor is attracting interest in drug discovery for the development of new chemical entities producing analgesia with minimal adverse effects.

Structure-activity relationship (SAR) studies have shown that the C-terminal NT(8–13) fragment retains the full biological activity of NT, thereby defining it as the essential amino acid sequence for the development of NT(8–13)-based analgesics [41]. Since then, several NT (8–13) analogs harboring reduced amine bonds and site-specifically modified unnatural amino acids have been developed to improve receptor binding affinity, subtype selectivity, efficacy/potency and peptide stability. Among these compounds, NTS1-selective agonists (PD149163 and NT72) were reported to induce antinociceptive effects following central administration [31,32,42–44]. Likewise, centrally injected NTS2-selective analogs (JMV431 and NT79) have been shown to successfully reverse nociceptive behaviors in both acute and chronic pain models [23,26,33,45–47].

In recent years, the drug development of peptide therapeutics has received renewed interest from the pharmaceutical industry. To date, over 50 peptide drugs targeting GPCRs have been approved by the FDA for clinical use, most of them for the treatment of type 2 diabetes mellitus and other metabolic disorders, as well as oncology indications [48]. Among the chemical strategies used to optimize the properties of NT (8–13), peptide cyclization has shown great success in improving the physicochemical properties of active NT analogs targeting NTS1 [49,50]. Indeed, macrocyclization often increases proteolytic stability through restricted accessibility to the cleavage sites [51–53]. Furthermore, cyclization allows control of the peptide conformation and thus mimics secondary structures and improves ligand-receptor binding. Macrocyclic compounds thus combine the ability to present remote pharmacophores while maintaining a semirigid structure [51]. In addition, macrocycles that possess better absorption, distribution, metabolism, and excretion/pharmacokinetics (ADME/PK) properties may display an increased ability to cross barriers, as evidenced by the cyclic NT(8–13) nonselective analog (JMV2012) exhibiting central bioavailability [54]. Ring size is also an important factor when considering an appropriate synthesis strategy. Therefore, we recently reported the optimal macrocyclization site for NT(8–13) and a potent new NT (8–13) macrocyclic scaffold [49,50]. This macrocyclic compound displayed an excellent affinity for NTS1, as well as potent analgesia. As expected, however, it was associated with hypothermia and hypotension.

Here, we describe the synthesis and in vitro/in vivo characterization of the first constrained NTS2 macrocyclic NT(8–13) analog. The Tyr^{11} residue of NT(8–13), which was previously reported in linear peptides to play a critical role in receptor subtype selectivity [23,45,46,55–61], was replaced with a Trp^{11} followed by side-chain to side-chain macrocyclization between Lys^{8} and Trp^{11}. The pharmacodynamic and pharmacokinetic properties of the resulting constrained NT(8–13) macrocyclic compound, designated CR-01-64, were then assessed, with a particular emphasis on antinociceptive activity, interactions with the opioid system and potential NT-related adverse effects.

2. Materials and methods

2.1. Peptide synthesis

All peptides were synthesized on a 50 μmol scale using 2-chlorotrityl chloride resin from Matrix Innovation (maximum loading 0,89 mmol/g). Commercially available Fmoc-protected amino acids were purchased from Chem-Impex, Matrix Innovation and Sigma-Aldrich at >95% purity. Amino acid coupling was performed on an orbital shaker at 150 RPM using 6 mL of solid-phase synthesis reactors equipped with a 20 μm frit from Applied Separations.

2.1.1. Standard resin washing procedures

The resin was washed using a standard sequence of DMF, DCM, iPrOH, DCM, and DMF, with ~3 mL of solvent per reactor in each wash. When a dried resin was required, two additional washes with DCM were performed.

2.1.2. Resin loading

Standard 2-chlorotrityl chloride resin was allowed to react with 4 mL of DCM containing 0.5 mmol/g of the first amino acid and 1,5 eq. of DIPEA for at least 2 h. The resin was then washed using the standard procedure described above. Unreacted chlorotrityl sites were capped using a 7/2/1 solution of DCM/methanol/DIPEA for at least 20 min. When loading was uncertain, 10 mg of the loaded resin were isolated and deprotected using 2 mL of 20% piperidine in DMF for 10 min. A spectrophotometric analysis of the supernatant was performed to estimate the dibenzofulvene concentration, which reflects amino acid loading.

2.1.3. Fmoc deprotection

Fmoc-protected peptides were deprotected in the solid phase using piperidine 20% v/v in DMF for 5 min, and this step was repeated once. Standard wash procedures were subsequently performed.

2.1.4. Coupling of amino acids

When coupling commercially available and inexpensive amino acids, 5 eq. were reacted with 5 eq. of HATU and 6 eq. of DIPEA in 4 mL of DMF. The reaction mixture was stirred on an orbital shaker for at least 20 min. Standard wash procedures were then applied.

2.1.5. Coupling of expensive amino acids

Expensive amino acids were coupled using 2 eq. amino acid in the presence of 2 eq. of HATU and 3 eq. of DIPEA in 4 mL of DMF. The reaction mixture was stirred on an orbital shaker for at least 2 h. Standard wash procedures were then applied.

2.1.6. Synthesis of unnatural Fmoc-Trp(N-Allyl)-OH

2.1.6.1. Boc-Trp-OMe. Triethylamine (5,75 mL, 41,2 mmol) was added to flame-dried RBF with L-Trp methyl ester HCl (10 g, 39.3 mmol) in THF (100 mL) under Ar and cooled on ice. Di-tert-butyl dicarbonate (9 g, 41,2 mmol) in THF (40 mL) was subsequently added slowly. The reaction mixture was stirred at room temperature overnight. The product was then evaporated under vacuum and partitioned in 50:50 AcOEt: H2O. The organic phase was washed with water once and brine twice,

dried with MgSO4 and evaporated under a vacuum. Purity was confirmed using TLC. Flash chromatography was not performed (100% conversion via TLC).

2.1.6.2. Boc-Trp(N-Allyl)-OMe. Cesium carbonate (12.4 g, 37.7 mmol) was added to a solution of Boc-Trp methyl ester (3.33 g, 10.4 mmol) in DMF (~22 mL) in a pressurized vessel and stirred for 2–3 min. Allyl bromide (2.71 mL, 31.3 mmol) was then added slowly, and the reaction mixture was stirred at 90 °C for 4 h until the disappearance of the starting material was detected using TLC. After cooling to room temperature, the solvent was evaporated overnight under airflow. The crude product was solubilized in DCM with a small amount of AcOEt and purified using flash chromatography on silica gel 20% AcOEt:hexanes, yielding 2.98 g of N_a-Boc-N_{ind}-AllylTrp-OMe as a slightly yellow oil.

2.1.6.3. Boc-Trp(N-Allyl)-OH. Lithium hydroxide (1.19 g, 49.9 mmol) in H_2O (~35 mL) was added to a solution of N_a-Boc-N_{ind}-AllylTrp-OMe (2.98 g, 8.31 mmol) in THF (20 mL). The reaction mixture was stirred at room temperature for 30 min until TLC indicated complete conversion (3:7 AcOEt:hexanes with 1% acetic acid). THF was then evaporated under reduced pressure. The solution was acidified using 1 M HCl, AcOEt was added, and the organic phase was washed with water and brine. The organic layer was dried over Na_2SO_4 and concentrated to yield 2.98 g of N_a-Boc-N_{ind}-AllylTrp-OH as a colorless oil. The product was not purified.

2.1.6.4. Trp(N-Allyl)-OH. A TFA/TIPS/H_2O mixture with a 95/2.5/2.5 vol ratio (~30 mL) was added to N_a-Boc-N_{ind}-AllylTrp-OH (2.98 g, 8.65 mmol) and stirred for 30 min to completion, as assessed using TLC. The solution was evaporated and diluted with DCM for 3 subsequent co-evaporations to remove all TFAs. The product was not purified.

2.1.6.5. Fmoc-Trp(N-Allyl)-OH. N_{ind}-AllylTrp-OH (2.11 g, 8.64 mmol) was dissolved in H_2O and THF (~50 mL of both) at a pH adjusted to 7–8 using sodium bicarbonate. Fmoc chloride (2.31 g, 8.84 mmol) was dissolved in THF (~15 mL), and both solutions were combined, with the pH observed and adjusted during the reaction accordingly to maintain it at approximately 7–8. After 3 h of stirring, THF was evaporated, and the solution was extracted with Et_2O three times. Then, the pH of the aqueous solution was adjusted to 2 using 1 N HCl before washing with EtOAc until extraction was complete, as assessed using TLC. EtOAc fractions were combined, washed with brine, dried with Na_2SO_4 and evaporated. Biotage chromatography of 3.109 g of the crude product yielded 1.120 g of N_a-Fmoc-N_{ind}-AllylTrp-OH.

2.1.7. Ring-closing metathesis

The dried resin (200 mg) and 0.2 eq of Grubbs-Hoveyda 2nd generation (6.3 mg, 0.01 mmol) were added to a flame-dried, argon-filled microwave tube containing a stir bar. The resin and catalyst were degassed for 10 min under an argon flow and were then suspended in 3 mL of anhydrous dichloroethane. The reaction mixture was then heated in a CEM Discover microwave for 1 h at 70 °C. Standard wash procedures were applied.

2.1.8. Simultaneous cleavage of the resin and Boc-protected groups

A solution of 95/2,5/2,5% TFA/TIPS/H_2O (~2.5 mL) was added to the dried resin described above and allowed to react for 2 h on an orbital shaker. The acidic solution was filtered, and the filtrate was poured into ~10 mL of *tert*-butyl methyl ether. The solution was centrifuged at 3000 RPM at 4 °C for 10 min, and the supernatant was analyzed using UPLC-MS to confirm the absence of the peptide and then discarded. If the peptide was still present, the supernatant was either evaporated and copurified with the precipitate or extracted with 3:1 water/ACN, lyophilized and then purified with the crude material. The precipitate was subsequently evaporated in vacuo.

2.2. Peptide purification

The dried crude mixture obtained in the previous step was solubilized in a 1:1 ACN/H_2O mixture (1–1.8 mL) and purified on a Waters preparative HPLC-MS column (XSELECTTM CSHTM Prep C18 (19 × 100 mm) packed with 5 μm particles, UV detector 2998, MS SQ Detector 2, Sample manager 2767 and a binary gradient module). The eluents used were acetonitrile to which 0,03% aqueous ammonia was added, as well as water with 20 mM NH_4CO_3.

First, a 10-min run was performed with the eluents listed above and a gradient of 5% ACN to 95% ACN (0–10 min) to estimate the %ACN where the product was eluted. A second run was performed using the following eluent program: [(%ACN) - 10 - (%ACN) + 5] (0–15 min). Fractions collected were analyzed on a Waters UPLC-MS system (column Acquity UPLC® CSHTM C18 (2.1 × 50 mm) packed with 1.7 μm particles) using ACN and water + 0,1% formic acid. The separation method used in this step was 0–0.2 min: 5% ACN; 0.2–1.5 min: 5–95% ACN; 1.5–1.8 min: 95% ACN; 1.8–2.0 min: 95–5% ACN; 2.0–2.5 min: 5% ACN. Pure fractions were grouped and lyophilized. HRMS spectra of the peptides were also recorded using a maXis ESI-Q-TOF in ESI+ mode.

2.3. Competitive radioligand binding assay using hNTS1 and hNTS2 receptors

CHO-K1 cells stably expressing hNTS1 (ES-690-C from PerkinElmer, Montréal, Canada) or 1321N1 cells stably expressing hNTS2 (ES-691-C from PerkinElmer, Montréal, Canada) were cultured in DMEM/F12 at 37 °C in a humidified chamber with a 5% CO_2 atmosphere. Culture media were supplemented with 10% FBS, 100 U/mL penicillin, 100 μg/mL streptomycin, 20 mM HEPES, and 0.4 mg/mL G418. Cells expressing hNTS1 were frozen when they reached 80% confluence. They were scraped off the dish in 10 mM Tris buffer and 1 mM EDTA, pH 7.5, and centrifuged at 15,000 g for 5 min at 4 °C. The pellet was then resuspended in 1 mL of binding buffer. Cells expressing hNTS2 were also frozen when they reached 80% confluence. They were scraped off the dish in PBS and 0.5 mM EDTA, pH 7.5, and sonicated for 5 min (pulse 30 s/5 s off, amplitude 40%). They were ultracentrifuged at 100,000 g for 60 min at 4 °C. The pellet was resuspended in 1 mL of freezing buffer (PBS, glycerol, and 0.5 mM EDTA), sonicated for 1 min (pulse 30 s/5 s off, amplitude 50%) and further diluted in binding buffer. Competitive radioligand binding experiments were performed by incubating 15 μg of cell membranes expressing the hNTS1 receptor with 45 pM ^{125}I-[Tyr^3]-NT (2200 Ci/mmol) or 50 μg of cell membranes expressing the hNTS2 receptor with 300 pM ^{125}I-[Tyr^3]-NT in binding buffer (50 mM Tris-HCl, pH 7.5, 0.2% BSA). The samples were incubated with increasing concentrations of analogs ranging from 10^{-11} to 10^{-4} M for 60 min at 25 °C, and then, the binding reaction mixture was transferred to PEI-coated 96-well filter plates (glass fiber filters GF/B, Millipore, Billerica, MA). The reaction was terminated by filtration, and the plates were washed three times with 200 μL of ice-cold binding buffer. Glass filters were then counted using a γ-counter (2470 Wizard2, PerkinElmer, Mississauga, Ontario, Canada). Nonspecific binding was measured in the presence of 10^{-5} M unlabeled NT(8–13) and represented less than 5% of total binding. Data for NT(8–13) were normalized to the control to exclude unwanted sources of variation. IC_{50} values were determined from competition curves as the unlabeled ligand concentration inhibiting 50% of ^{125}I-[Tyr^3]-NT-specific binding. K_i values were determined using the Cheng-Prusoff equation from IC_{50} values [62]. Competitive radioligand binding data were plotted using the nonlinear regression One-site-Fit log(IC_{50}) and presented the means ± SEM of three independent experiments, each performed in triplicate. The binding assay was performed in triplicate to ensure the reliability of single values.

2.4. Plasma and cerebrospinal fluid (CSF) stability assays

Rats were anesthetized with 2.5% isoflurane for blood collection and

with ketamine/xylazine (87 mg/kg: 13 mg/kg, i.m.) for CSF collection. Rat plasma was obtained by centrifuging blood at 13,000 rpm for 5 min at 4 °C. Rat CSF was collected from the cisterna magna. Six microliters of a 1 mM aqueous solution of the peptide was incubated with 27 µL of rat plasma or rat CSF at 37 °C for 24 h (or for 1, 2, 3 and 5 min for NT(8–13) in plasma and for 8, 16 and 24 h for NT(8–13) in CSF). Proteolytic degradation was quenched by adding 70 µL of a 10% trichloroacetic acid and 0.5% nicotinamide solution followed by immediate vortexing. Samples were centrifuged (13,000 rpm, 5 min, 4 °C), and the supernatant was filtered through a 4 mm nylon 0.2 µm syringe filter and then analyzed using UPLC-MS (Waters 2695 with ACE C18 column 2.0 × 100 mm, 2.7 µm spherical particle size and Electrospray micromass ZQ-2000 from Waters). Data were analyzed with GraphPad Prism 7 software using a one-phase decay equation and presented as the half-life from three independent experiments.

2.5. In vivo analgesic assay

2.5.1. Animals, housing and habituation

Experiments were performed with adult male Sprague-Dawley rats weighing 225–300 g (Charles River laboratories, St. Constant, Canada). Rats were housed in groups of two per cage on Aspen shavings in a quiet room, maintained on a 12 h light/dark cycle and allowed ad libitum access to food and water. All experimental procedures reported in this study were approved by the Animal Care Committee of Université de Sherbrooke in accordance with policies and directives of the Canadian Council on Animal Care. Furthermore, they were performed in agreement with the ARRIVE (Animals in Research: Reporting In Vivo Experiments) guidelines and the United States NIH [63].

2.5.2. Intrathecal administration

Rats were lightly anesthetized with a flow of 2% isoflurane (Baxter Corporation, Mississauga, ON, Canada) and oxygen (2 L/min) and injected intrathecally using a 27G needle at the L5-L6 intervertebral space with saline or the test compound diluted in 0.9% saline at concentrations ranging from 3 to 60 µg/kg.

2.5.3. Tail-flick test

Acute pain was assessed using the tail-flick test (Tail-Flick Analgesia meter V2.00, Columbus Instruments, Columbus, Ohio, USA), which measures heat-induced pain in animals and is reflective of injected compound analgesic efficacy [64]. The test measures sensitivity to a high-intensity light beam focused on the rat's tail. The tail-flick apparatus was set at a light intensity of 6, and a cutoff of 10 s was used. Testing involved measurements of the latency for the rat to withdraw its tail from the path of the light beam, which corresponds to the measure of pain sensitivity. Before testing, animals were individually acclimatized to manipulations and the behavioral apparatus 5 min/day for three consecutive days. On the test day, a latency baseline was recorded before the drug injection. The compound was diluted in 0.9% saline and injected at increasing doses ranging from 3 to 60 µg/kg. Morphine was injected intrathecally at an equimolar dose to CR-01-64 (30 µg/kg = 35 nmol/kg) or intravenously at 1 mg/kg, alone or in combination with CR-01-64 at 30 µg/kg. The NTS2 antagonist NTRC-844 was diluted in DMSO and was injected intrathecally at a 10x equimolar dose to CR-01-64 (350 nmol/kg), alone or in combination with CR-01-64 at 30 µg/kg. Naloxone was injected intraperitoneally at 10 mg/kg 30 min before the administration of CR-01-64. The effects of the compound or saline on thermal nociception were assessed every 10 min for up to 60 min following i.t. administration. Tail-flick latency was then converted into the percent maximal possible effect (% MPE) at the time of maximal peak of analgesia. % MPE was calculated according to the following formula: %MPE = [(Test latency) – (Saline latency)]/[(Cutoff) – (Saline latency)] × 100. Data are presented as the means ± SEM of 6 animals for each treatment dose. The half-maximal effective dose (ED_{50}) of the compound was determined based on the % MPE at 20 min, which was calculated for each dose in the tail-flick test. Then, ED_{50} values were determined using the dose-response stimulation log(agonist) vs response (four parameters).

2.5.4. Formalin test

The analgesic effects of compounds were assessed using the formalin test as a model of persistent pain. Before testing, animals were acclimatized to manipulations and the experimental apparatus for three consecutive days (30 min/day). On the test day, 5 min after intrathecal injection of the compound at increasing doses ranging from 3 to 60 µg/kg, rats received a subcutaneous injection of 50 µL of diluted formaldehyde (1.85%; i.e., 5% formalin; Bioshop, Burlington, Ontario) into the plantar surface of the right hind paw. Rats were then placed in clear Plexiglas chambers (30 × 30 × 30 cm) positioned over a mirror angled at 45° to allow an unobstructed view of the rats' paws. Their behavior was then observed for the next 60 min. The intraplantar injection of formalin produced a biphasic nociceptive response typical of this tonic pain model [65]. The two distinct phases of spontaneous pain behaviors that occur in rodents are proposed to reflect first the direct effect of formalin on sensory receptors (acute phase, 0–9 min) and longer-lasting pain due to inflammation and central sensitization (inflammatory phase, 21–60 min). Following the injection of formalin, mean nociceptive scores were determined for each 3 min block of the 60 min period by measuring the amount of time spent in each of four behavioral categories, as previously described [66,67]: 0, the injected paw is comparable to the contralateral paw; 1, the injected paw has little or no weight placed on it but still touches the ground; 2, the injected paw is elevated and is not in contact with any surface; 3, the injected paw is licked, bitten, or shaken. Behaviors believed to represent higher levels of pain intensity were given higher weighted scores. The weighted average pain intensity score ranging from 0 to 3 was then calculated by multiplying the time spent in each category by the category weight, summing these products, and dividing by the total time in a particular time interval. The pain score was thus calculated using the following formula (1T1 + 2T2 + 3T3)/180, where T1, T2, and T3 are the duration (in seconds) spent in behavioral categories 1, 2, or 3, respectively, during each 180 s block. The area under the curve (AUC) was calculated for all durations of the test (0–60 min). Data are presented as the means ± SEM of 5 rats treated with each dose.

2.5.5. Complete Freund's adjuvant-induced chronic inflammatory pain

The von Frey test was used to measure mechanical allodynia in a complete Freund's adjuvant (CFA)-induced chronic inflammatory pain model. Chronic inflammatory pain was induced with an intraplantar injection of 100 µL of CFA into the plantar surface of the rat's left hind paw. The injected volume (injected as a 1:1 emulsion of oil and saline 0.9%) contained the equivalent of 200 µg of lyophilized bacterial membranes (*Mycobacterium butyricum*) for a final concentration of 8 mg/mL. An intraplantar injection of saline 0.9% was administered to sham animals. CFA injections were performed under isoflurane/oxygen anesthesia. Rats were acclimatized to the Plexiglas enclosures, the mesh floor and the filament for 3 days prior to testing. On test days, rats were allowed 10 min to habituate to the enclosures. The von Frey test was performed before (day 0) and 3, 7 and 14 days after the CFA injection. Allodynia was determined using calibrated von Frey hairs. The blunt filaments were applied against the mid-plantar surface of the animal's hind paw. Filaments with increasing resistance were used, ranging from 2 to 15 g of force. The paw withdrawal threshold (PWT) was then determined, as previously described [68]. Fifty grams were considered the upper cutoff. Five values were recorded alternately for both ipsilateral and contralateral hind paws at intervals of 7 s. The effect of a 60 µg/kg dose of the compound or saline on allodynia was assessed at 15, 30, 60 and 120 min following i.t. administration on days 7 and 14. The % antiallodynic effect was calculated using the following formula: % antiallodynic effect = 100 × ($PWT_{compound}$ - PWT_{saline})/(PWT_{sham} - PWT_{saline}). Data are presented as the means ± SEM of 6 rats per

condition.

2.6. Body temperature measurement

Body temperature was measured using a thermistor probe inserted into the rat's rectum. Animals were individually acclimatized to manipulations and thermistor probes for three consecutive days. On the test day, temperatures were measured before (baseline) and every 10 min for up to 60 min following intrathecal drug administration. The compound was dissolved in 0.9% saline and injected at the highest dose of 60 μg/kg. Changes in body temperature (Δ body temperature) were determined from the baseline for each time point and each animal. Data are presented as the means ± SEM of 6 rats per condition.

2.7. Blood pressure measurement

Rats were anesthetized with ketamine/xylazine (87 mg/kg: 13 mg/kg, i.m.) and placed in a supine position on a heating pad. Mean, systolic and diastolic arterial blood pressure and heart rate were measured through a catheter (PE 50 filled with heparinized saline) inserted into the right carotid artery and connected to a Micro-Med transducer (model TDX-300, USA) linked to a blood pressure Micro-Med analyzer (model BPA-100c). Another catheter (PE 10 filled with heparinized saline) was inserted in the left jugular vein to administer bolus injections of the compound at 0.01 and 0.1 mg/kg (volume 1 mL/kg, over 5–10 s) or 0.9% saline. Blood pressure was recorded each second for up to 1000 s following the intravenous injection. Changes in mean arterial blood pressure (ΔMABP) were determined from the basal pressure of rats. Data are presented as the means ± SEM of 5 rats per condition.

2.8. Ex vivo ileum relaxation assay

Smooth muscle relaxation assays of the distal rat ileum were performed in isolated organ baths. Male Sprague-Dawley rats were anesthetized with an intramuscular injection of ketamine/xylazine (87 mg/kg: 13 mg/kg, i.m.) and euthanized by surgical rupture of the abdominal aorta. Tissues were rapidly removed, cut into 1 cm-long strips, cleaned of fat and feces, and mounted vertically in 15 mL baths. The baths were filled with oxygenated (95% O_2 and 5% CO_2) and thermoregulated (37 °C) Krebs solution (NaCl 118.1 mmol/L, KCl 4.7 mmol/L, $CaCl_2$ 2.5 mmol/L, KH_2PO_4 1.2 mmol/L, $MgSO_4$ 1.2 mmol/L, $NaHCO_3$ 25 mmol/L, and D-glucose 5.5 mmol/L; pH 7.4). Strips were stretched with a resting tension of 1.0 g followed by an equilibration period of at least 60 min with replacement of the Krebs solution every 15 min. At the beginning of each experiment, ileum preparations were challenged with 100 nM carbachol until a constant contractile response was achieved, with multiple washes between stimulations. Tissues were then precontracted with the same dose of carbachol and presented analog concentrations ranging from 10^{-11} to 10^{-5} M. Noncumulative concentration-response curves were established; thus, analogs were added to the baths as a single addition following washout of the previous dose. Muscular contractions were measured isometrically with force transducers (Radnoti Glass Technology Inc.) and recorded on multichannel chart recorders (PowerLab 8/30, ADInstruments) linked to LabChart Pro software (version 8.1.8). The percentage of ileum relaxation was calculated for each individual contraction. EC_{50} values were determined by calculating the dose response – stimulation Log(agonist) vs. response (four parameters) - using GraphPad Prism 7 and presented as the means ± SEM of three different experiments.

2.9. In vivo pharmacokinetics (PK)

2.9.1. Blood PK

On the day before the experiment, animals were anesthetized with ketamine/xylazine (87 mg/kg: 13 mg/kg, i.m.) and placed in a supine position on a heating pad. The jugular vein was catheterized using 20 cm silastic tubing, with external and internal diameters of 0.96 and 0.58 mm, respectively (Becton Dickinson, Franklin Lake, NJ, USA). The catheter was subcutaneously tunneled and fixed at the back of the neck. Heparinized saline (100 UI/mL) was injected into the catheter to avoid thrombosis and catheter obstruction, and the wound was closed. Rats were then returned to their individual cages for a recovery period of at least 24 h, allowing complete anesthesia washout. On the day of experimentation, rats were placed in horizontal Plexiglas cylinders (6.5 cm internal diameter, up to 20 cm adjustable length) (Harvard Apparatus, Inc., Holliston, MA, USA). Following an i.v. injection of 0.2 mg/kg CR-01-64, 300 μL of blood were sampled from catheterized rats at 5, 10, 15, 30, 60, and 120 min postinjection. Blood samples were collected in Eppendorf tubes containing 30 μL of sodium heparin (Sandoz, Boucherville, Canada). After centrifugation (5000 rpm, 10 min), plasma was isolated and stored at −80 °C until analysis.

2.9.2. Cerebrospinal fluid PK

Rats received an i.t. injection of 60 μg/kg CR-01-64 diluted in 0,9% NaCl. Shortly before sampling, rats were deeply anesthetized with ketamine/xylazine (87 mg/kg: 13 mg/kg, i.m.) and fixed on a stereotaxic frame using ear bars. The head was maintained downward at approximately 45° to place the cisterna magna in the proper position [69]. A 27G winged perfusion needle connected to a syringe was inserted into the cisterna magna. Approximately 150 μL of cerebrospinal fluid (CSF) were then collected at 10, 30, 60, 90, 120, 180, 240, 360 or 480 min after the CR-01-64 injection. Only one CSF sample was collected from each rat, and three replicates were performed for each sampling time. Rats were then euthanized, and CSF samples were stored at −80 °C until analysis.

2.9.3. Measurements of CR-01-64 concentrations in plasma and CSF

The CR-01-64 concentration was analyzed using a Sciex Qtrap 6500+ mass spectrometer (Ab Sciex LLC, Framingham, MA, USA) coupled to a microflow M3 liquid chromatography apparatus equipped with an HSST3 column (100 mm × 1 mm, 1.8 μm equipped with a 0.2 mm fritted prefilter). The solvent flow rate was set to 50 μL/min, and the column temperature was maintained at 35 °C. The sample volume injected was 2 μL. The mobile phase was 0.10% formic acid/water (A) and 0.10% formic acid/methanol (B). The elution gradient started with 5% eluent B for 1 min, increased to 10% in 2.5 min, and then increased to 20% over 3.5 min. Solvent B was then pumped up to 95% over 1 min and held at that concentration for 2 min. It was then increased to 100% over 1 min and held at that concentration for 3 min. The initial solvent mixture was then re-established over 1 min and held for 2 min. The equilibration time was 3 min, and the total run time was 16 min. Mass spectrometry analysis was performed using a positive electrospray ionization (ESI+) source in multiple reaction monitoring mode (MRM). The optimized parameters were obtained by directly infusing the analytical standard solution at 10 ng/mL as follows: CUR at 30; Caz 1 at 20; capillary voltage of 5.5 kV; source temperature of 150 °C and desolvation temperature of 350 °C. Two product ions (transitions) were used; the most abundant transition was used for quantification, whereas the second most abundant transition was used for qualification. MS/MS acquisition and data processing were performed with Analyste 1.6.3, and quantification was performed with multiquad software from Sciex LLC.

2.9.4. Plasma and CSF PK analyses

Plasma and CSF PK were analyzed using Phoenix WinNonlin (Certara, Princeton, NJ, USA). Plasma CR-01-64 PK parameters were assessed after the i.v. injection using a two-compartmental model with a first-order elimination including the initial plasma concentration (C_0), central volume of distribution (V_1), elimination rate constant (k_{10}), transfer rate constants between central and peripheral compartments (k_{12} and k_{21}), volume of distribution at steady state (V_{SS}), total clearance (Cl), distribution and elimination rate constants (α and β), distribution

and elimination half-life ($t_{1/2}\alpha$ and $t_{1/2}\beta$) mean residence time (MRT) and area under the concentration-time curve (AUC_{inf}). CSF CR-01-64 PK parameters were assessed after the i.t. injection using a non-compartmental analysis including the peak plasma concentration (C_{max}), time to achieve C_{max} (T_{max}), terminal elimination rate constant (λz), elimination half-life ($t_{1/2}\ \lambda z$), volume of distribution (V_Z/F), total clearance (Cl_Z/F), mean residence time (MRT) and area under the concentration-time curve (AUC_{last}).

2.10. Data and statistical analysis

All experimental protocols, data, and statistical analyses described in this study comply with the recommendations on experimental design and analysis in pharmacology [70]. Animals were randomized to treatment groups, and binding experiments were performed by investigators who were blinded to the compound. Reference compounds were tested by several experimenters to avoid potential bias in the assessment of pain, with consistent results.

For the behavioral tests, baseline latency in the tail-flick test, AUC of the pain scores in the formalin test and baseline paw withdrawal threshold on days 7 and 14 in the von Frey test followed a normal (or Gaussian) distribution, as determined using the Shapiro-Wilk normality test. Parametric tests were then performed to increase statistical power. For ANOVA, post hoc tests were conducted only if F was significant and no variance in homogeneity was detected. Data are presented as the means ± SEM (or means ± SD for PK studies). All graphs and statistical analyses were performed using GraphPad Prism 9 (GraphPad software, La Jolla, CA, USA). Two-way ANOVA followed by Dunnett's multiple comparison test was used to determine differences in the tail-flick latency, paw withdrawal threshold and body temperature between the saline-treated group and groups treated with different doses of CR-01-64 or different compounds at equimolar doses (*), between groups coadministered CR-01-64+ morphine and morphine ($) or CR-01-64 (!), or between groups administered CR-01-64 and morphine (?), or to determine differences in paw withdrawal threshold between sham and saline groups (#). The %MPE and AUC for the formalin test and % anti-allodynic effect were analyzed using one-way ANOVA followed by Dunnett's multiple comparison test to compare the effect of saline treatment and different doses of CR-01-64. The %MPE in the acute pain model or the AUC in the tonic pain model were calculated for each dose of the compound to determine the half-maximal effective dose (ED_{50}) of CR-01-64. Then, ED_{50} values were determined using the dose-response stimulation log(agonist) vs response (three parameters). Nonlinear regression analyses using three parameters were also performed to determine the half-maximal inhibitory concentration (IC_{50}) of neurotensin in the ileum relaxation assay. For binding affinities, K_i values ± SEM were calculated from the IC_{50}, which were derived from the resulting dose-response curves. A difference in response between the compound and saline was considered significant with p-values of *$p < 0.05$, **$p < 0.01$, ***$p < 0.001$ and ****$p < 0.0001$. A difference in the response between sham animals and saline-treated animals was considered significant with a p-value ####$p < 0.0001$. A difference in the response between the CR-01-64 and morphine treatments was considered significant with the following p-values: ?$p < 0.05$, ??$p < 0.01$, and ???$p < 0.001$. A difference in the response between groups coadministered CR-01-64+ morphine and animals treated with morphine ($) or CR-01-64 (!) alone was considered significant with the following p-values: $$$p < 0.01$, $$$$p < 0.0001$, !$p < 0.05$, !!!$p < 0.001$, and !!!!$p < 0.0001$.

3. Results and discussion

3.1. Design and synthesis of a neurotensin receptor type 2 (NTS2) macrocyclic analog

Peptide-based therapeutics occupy a structural niche between the two main classes of available drugs: biologics and small molecules. Among the strategies used to improve peptide druggability, macrocyclization has been shown to be effective at providing suitable conformations for proper ligand-receptor interactions [51]. Peptide macrocyclization indeed increases the affinity and selectivity for a specific target, as well as the metabolic stability, permeability and pharmacokinetic properties [71,72]. The current pipeline of macrocycles includes over 80 approved drugs, with almost half of them belonging to the cyclic peptide class [72–74]. Among the well-known examples of cyclic peptide drugs on the market, eight currently target GPCRs. These drugs include somatostatin analogs targeting different SSTR subtypes (SSTR1, 2, 3 and 5), such as octreotide, lanreotide and pasireotide, which are used clinically as oncological drugs or to treat Cushing's disease and acromegaly; the synthetic analog of the vasopressin antidiuretic hormone desmopressin, which is administered orally or as an intranasal spray to treat diabetes insipidus, polydipsia and polyuria through its binding to V2 receptors; the synthetic oxytocin pitocin, which is used to stimulate uterine smooth muscle contractility during labor by binding to oxytocin receptors (OXTR); the cyclic peptide analog of α-MSH, bremelanotide, which primarily functions as an agonist of the melanocortin receptors MC3 and MC4 and is approved for sexual arousal disorder; and finally the calcitonin derivatives miacalcin and elcatonin that act on the amylin (AMY1) and calcitonin (CT) receptors, respectively, and are used to treat Paget disease, hypercalcemia and pain caused by osteoporosis. Importantly, several cyclic peptide drug candidates targeting other GPCRs are also in active clinical development. Among those candidates being investigated in ongoing phase III trials, balixafortide, a potent and highly selective bicyclic peptide antagonist of the CXCR4 chemokine receptor, is used to manage tumor growth and metastatic breast cancer. Motixafortide, which was developed to treat human cancers, specifically pancreatic cancer, is a cyclic synthetic peptide that also acts as a selective blocker of CXCR4. Livoletide, a first-in-class analog of ghrelin, is used to treat hyperphagia and obesity in patients with Prader-Willi syndrome, a rare genetic disease. Finally, setmelanotide, an MC4 cyclic agonist octapeptide, was developed as an anti-obesity medication.

Of particular importance, peptide cyclization has shown great success in generating active macrocyclic NT(8–13) analogs targeting NTS1 [54,75–78]. Accordingly, we have recently delineated the optimal ring size and macrocyclization sites for NT(8–13), leading to the development of high-affinity NTS1 cyclic agonists exhibiting better resistance to proteases [49,50]. In the present study, we focused on the design of NTS2-selective macrocyclic NT(8–13) peptides showing effective analgesia and few of the adverse effects of NT known to be related to NTS1 activation (i.e., hypotension, hypothermia and ileum relaxation). In this process, the Tyr^{11} residue of NT(8–13) was replaced with Trp^{11} to improve selectivity towards NTS2. Side-chain to side-chain macrocyclization was then performed using ring-closing metathesis (RCM) between Lys^8 and Trp^{11} to constrain the peptide conformation and improve its biological and metabolic properties. The resulting NT(8–13) macrocyclic peptide, designed CR-01-64, was synthetized using Fmoc-based solid phase peptide synthesis (SPPS) on 2-chlorotrityl chloride resin with standard procedures (Fig. 1) [49,50].

3.2. Pharmacodynamic profile of CR-01-64

3.2.1. CR-01-64 displays potent affinity and selectivity for NTS2

Dose-concentration displacement curves of [^{125}I]-neurotensin by CR-01-64 were generated using membranes prepared from cells stably expressing either hNTS1 or hNTS2 (Fig. 2). CR-01-64 displayed high affinity for NTS2 (K_i of 7.0 ± 2.9 nM), while the affinity for NTS1 was significantly decreased (871 ± 190 nM), thus yielding a macrocyclic compound showing 125-fold selectivity in binding affinity for NTS2. As NTS2-selective linear peptides were previously reported to induce analgesic responses in various animal pain models [23,26,33,44–47], we then decided to assess the analgesic effects of CR-01-64 on the responses

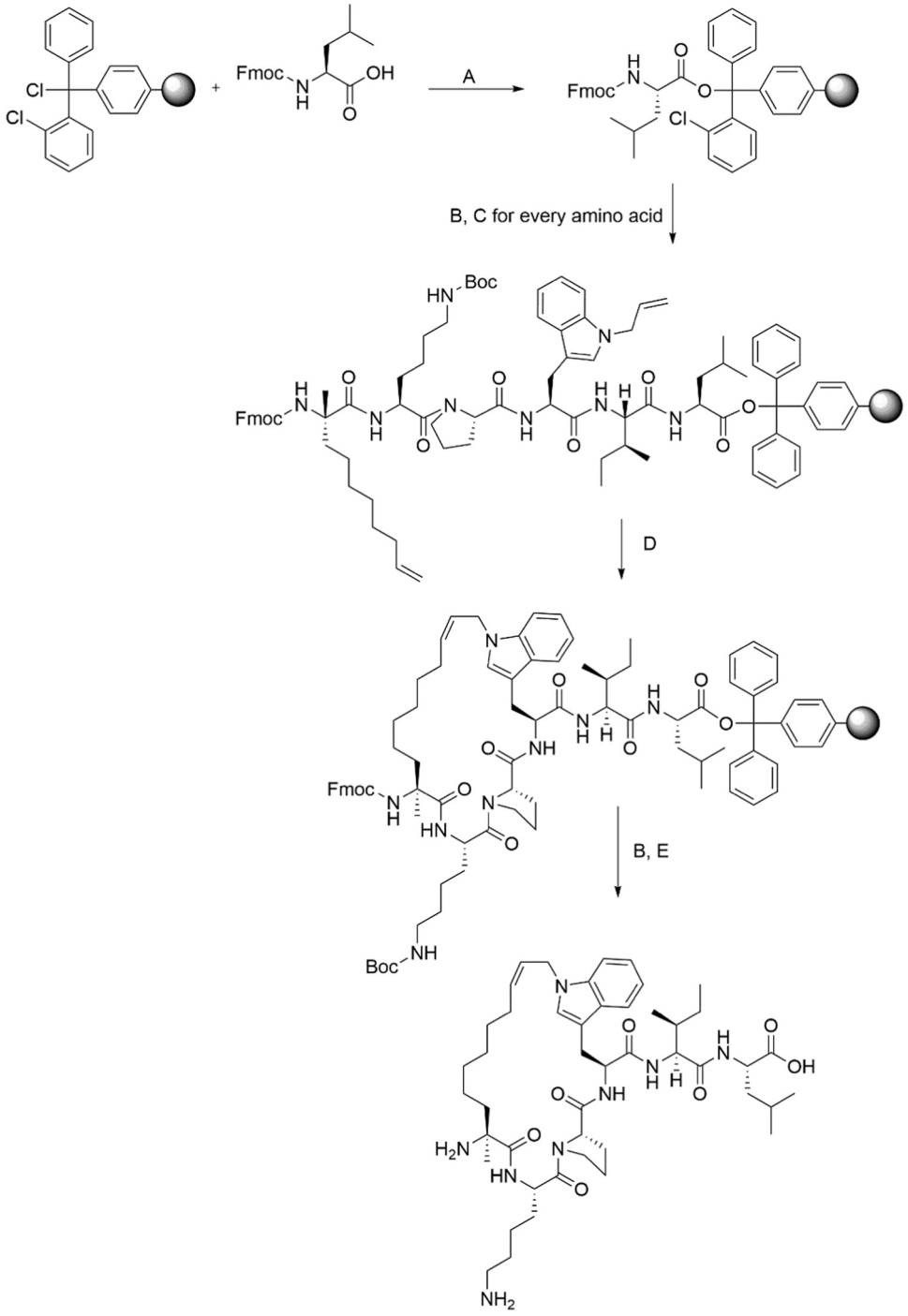

Fig. 1. Scheme of the synthesis of the NTS2 macrocyclic analog CR-01-64.

to thermal, chemical and mechanical pain stimuli in animal models of different experimental pain paradigms.

3.2.2. *In vivo analgesic activity*

3.2.2.1. CR-01-64 produces potent nonopioid antinociceptive effects and potentiates morphine-induced analgesia. The potential antinociceptive effect of CR-01-64 was first assessed using the radiant heat tail-flick test, which consists of measuring the withdrawal latency (rapid flick) to painful thermal stimuli applied to the tail. Intrathecal (i.t.) injections of CR-01-64 at doses ranging from 10 to 60 μg/kg significantly increased the tail-flick latency up to 40–50 min after administration compared to saline-treated rats (Fig. 3A). The calculated percentage of the maximum possible effect (% MPE) determined at 20 min postinjection revealed that CR-01-64 inhibited the nociceptive tail-flick reflex in a dose-dependent manner, reaching 95.4% inhibition at the highest dose tested (Fig. 3B). The resulting median effective analgesic dose (ED_{50}) was estimated to be 11.1 μg/kg (i.e., 13 nmol/kg; Fig. 3C). Importantly, coadministration with the selective NTS2 antagonist NTRC-844 completely abolished the analgesic effect of CR-01-64, indicating the sole role of the NTS2 receptor in CR-01-64-mediated analgesia (Fig. 3D) [79]. In this thermal acute nociceptive test, CR-01-64 provided pain relief similar to that provided by the previously described NTS2 analog JMV431 (Boc-Arg-Arg-Pro-Tyr-psi(CH2NH)Ile-Leu-OH) [33]. However,

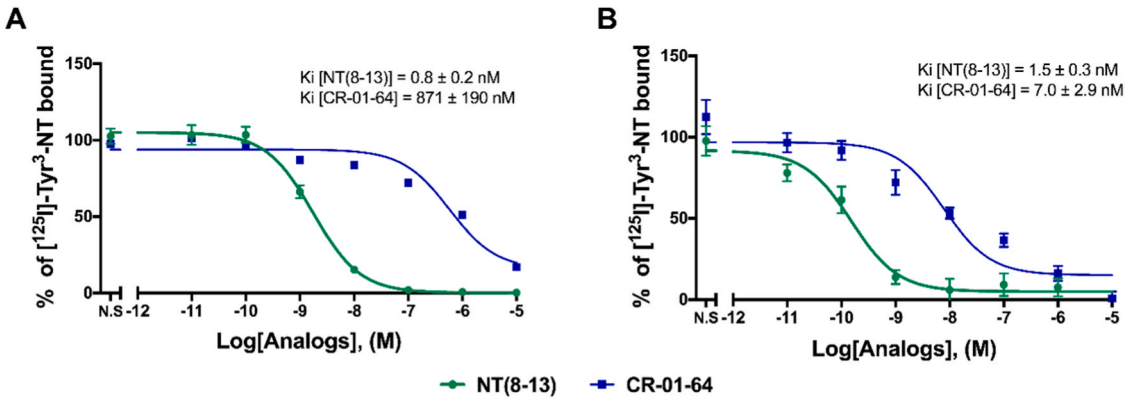

Fig. 2. Curves showing the displacement of [^{125}I]-neurotensin by NT(8–13) and CR-01-64 on hNTS1 (A) and hNTS2 receptors (B). Data are presented as the means ± SEM of at least three separate experiments.

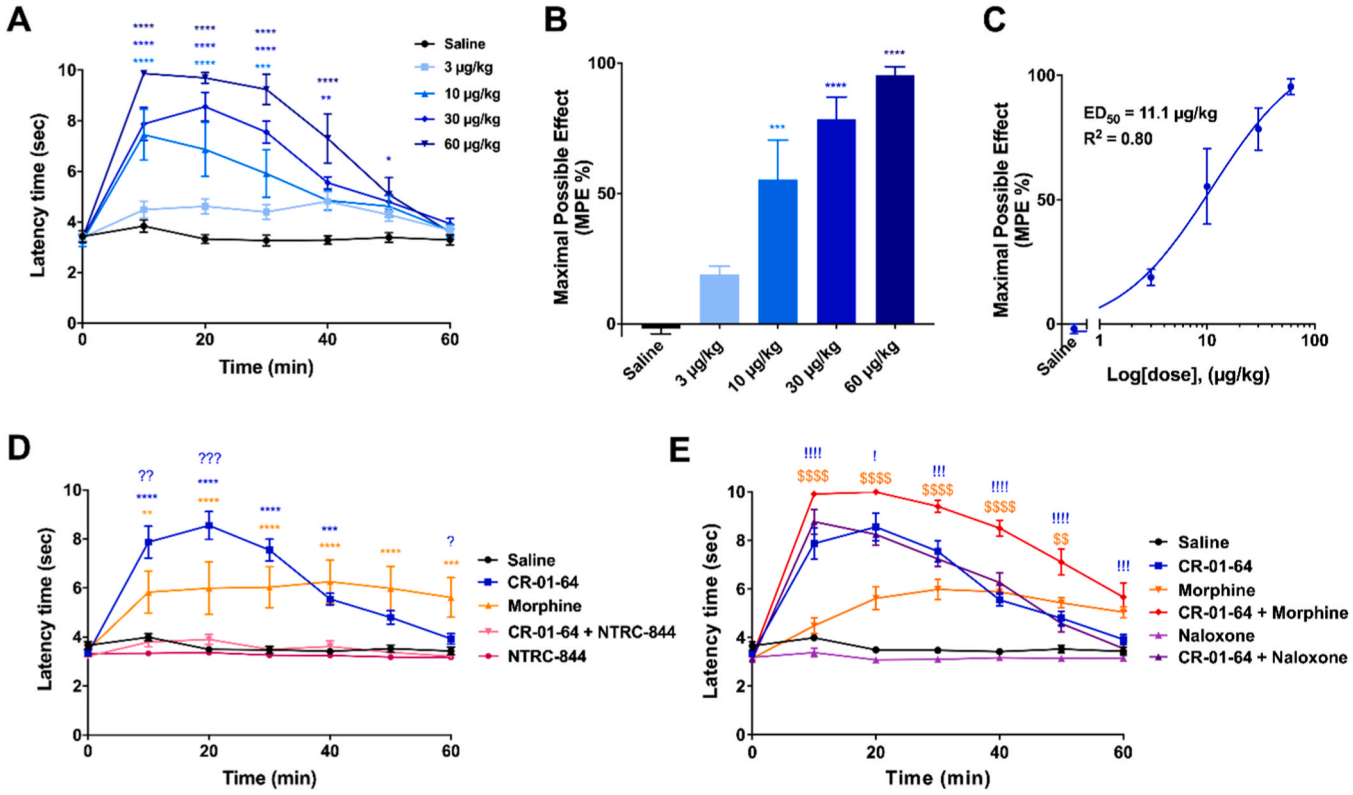

Fig. 3. Analgesic effect of CR-01-64 on tail-flick latencies in Sprague-Dawley rats. (A) Time course of the analgesic effect of an acute intrathecal injection of CR-01-64 at doses ranging from 3 to 60 µg/kg. (B) The percentage of maximal possible effect (%MPE) was calculated at 20 min postinjection, where the antinociceptive response was maximal for each dose. (C) Determination of the analgesic effective dose (ED_{50}) of CR-01-64. (D-E) Antagonism of the effect of the antinociceptive action of CR-01-64 by either NTRC-844 (NTS2 antagonist) or naloxone (µ-opioid antagonist). NTRC-844 was administered intrathecally at a 10× equimolar dose of CR-01-64, and naloxone was administered intraperitoneally at 10 mg/kg 30 min before the administration of CR-01-64. Comparison of the effects of CR-01-64, morphine, and their combination on acute pain. Morphine was administered intrathecally at an equimolar dose to CR-01-64 (30 µg/kg = 35 nmol/kg; D) or intravenously at 1 mg/kg (E). (A-D) Comparisons of the time courses for the effects of four doses of CR-01-64 and saline (*), between morphine and saline (*), and between CR-01-64 and morphine (?). (E) Comparisons of the time courses for the analgesic effects of CR-01-64+ morphine and morphine ($) or CR-01-64 (!). The results are presented as the means ± SEM (N = 6/group). For time courses (A, D, and E), comparisons were performed using two-way ANOVA with repeated measures followed by multiple comparisons using Dunnett's correction. For %MPE (B), comparisons were performed using one-way ANOVA with repeated measures followed by multiple comparisons using Dunnett's correction between groups treated with saline and CR-01-64 at different doses. Nonlinear regression analyses using three parameters were used to determine the dose-effect relationship. *$p < 0.05$, **$p < 0.01$, ***$p < 0.001$, ****$p < 0.0001$, $$$p < 0.01$, $$$$$p < 0.0001$, !$p < 0.05$, !!!$p < 0.001$, !!!!$p < 0.0001$, ?$p < 0.05$, ??$p < 0.01$, and ???$p < 0.001$.

CR-01-64 appeared to be approximately three times more potent than JMV431, which exhibits an ED_{50} of 33 nmol/kg. This increased potency might be due to the inherent properties of the macrocycle, which imposes a conformational constraint that potentially minimizes the binding entropy to achieve the most favorable conformation in the binding pocket of NTS2 [80]. We previously reported the synthesis and characterization of a series of nonselective NT(8–13) macrocyclic analogs formed via RCM between an ortho allylated tyrosine residue at position 11 and the side chain of an alkene-functionalized amino acid at position 8 of NT(8–13) [50]. The best compound of this series ([Orn

(All)-Lys-Pro-Tyr(OAll)]-Ile-Leu[13]), with an ED_{50} of 4.6 μg/kg, was less effective than CR-01-64, achieving 50% pain relief at the highest dose compared to 95.4% MPE for CR-01-64. Importantly, this macrocyclic analog also displayed a high binding affinity for NTS1 (K_i 15 nM) and therefore induced significant hypotensive and hypothermic effects, which limits its clinical use for pain management [50].

We next assessed the potential functional crosstalk between opioidergic and neurotensinergic systems. Indeed, compelling evidence has shown complex interactions between NT and opioid neurotransmission [4,9,81]. For instance, antisense peptide nucleic acids targeting the mu opioid receptor (MOR) do not affect the analgesic response to NT [82]. In contrast, we previously reported a significant decrease in morphine analgesia in NTS1-null mice [83]. In addition, a microinjection of MOR agonists in discrete brain regions produces antinociception by inducing NT release within the periaqueductal gray (PAG) [84,85]. Therefore, certain levels of interaction between opioid and NT systems and some uncertainty as to the NT receptor subtype involved in this cross-regulation exist.

In the tail-flick assay, despite its long-acting action, i.t. administration of an equimolar dose of morphine (35 nmol/kg), which is the gold standard opioid analgesic, was not as effective as CR-01-64 in increasing the withdrawal response latency to thermal nociceptive stimuli (Fig. 3D). This result is consistent with previous findings showing that NT-related compounds exhibit superior analgesic efficacy to equimolar doses of morphine in models of acute, tonic and neuropathic pain [23–26]. Of obvious importance is whether CR-01-64-induced analgesia was independent of the endogenous opioid system. Rats were pretreated with naloxone (10 mg/kg; i.p.) 30 min before the administration of

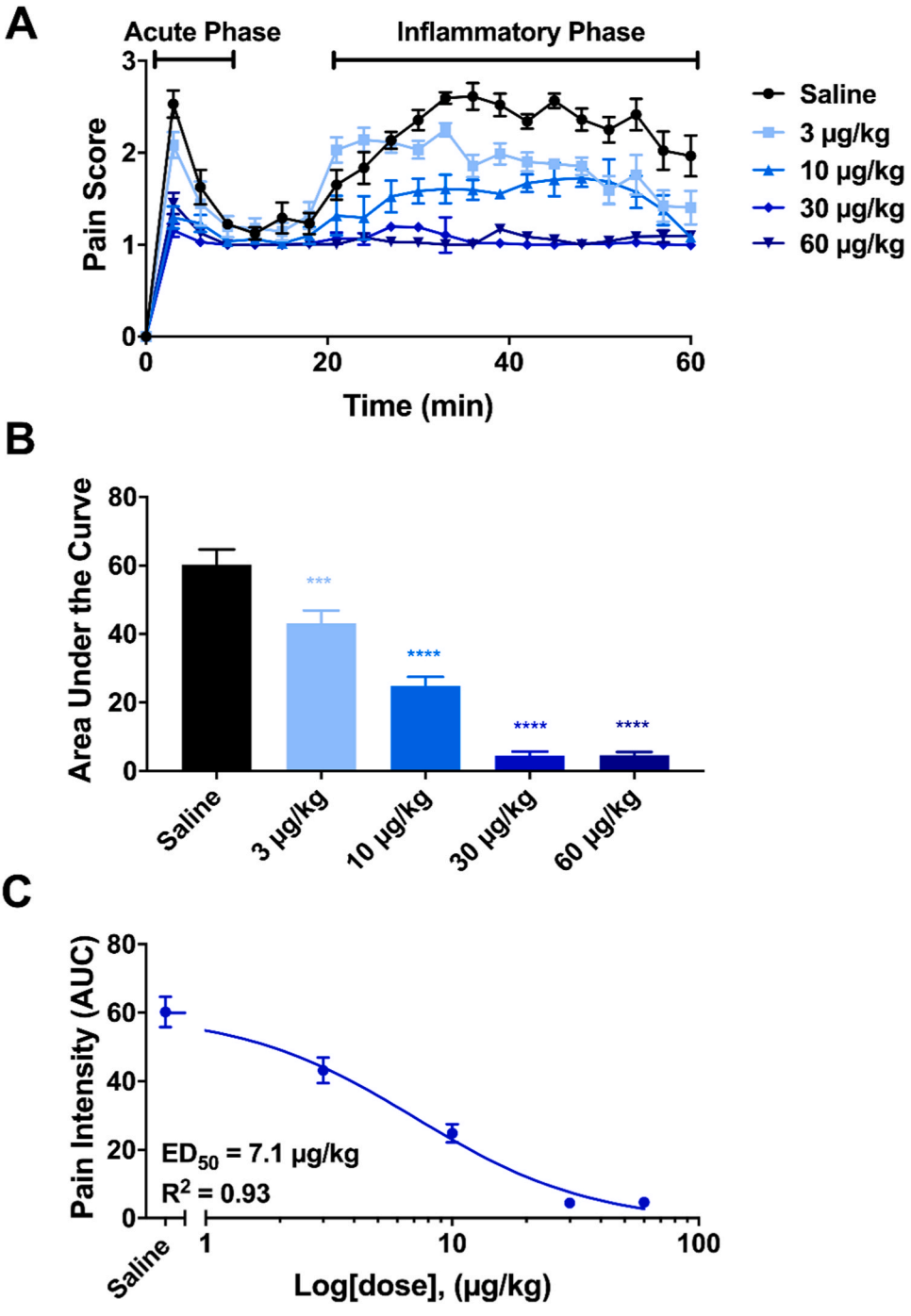

Fig. 4. Analgesic effect of an acute intrathecal injection of CR-01-64 on formalin-evoked pain-related behaviors in Sprague-Dawley rats. (A) Evaluation of the doses (from 3 to 60 μg/kg) inducing the antinociceptive effects of CR-01-64. (B) The area under the curve (AUC) was calculated for all durations of the test. (C) Determination of the analgesic effective dose (ED_{50}). The results are presented as the means ± SEM (N = 5/group). Comparisons between the AUCs of groups treated with saline and CR-01-64 at different doses were performed using one-way ANOVA with repeated measures followed by multiple comparisons using Dunnett's correction. Nonlinear regression analyses using three parameters were used to determine the dose-effect relationship. ***$p < 0.001$ and ****$p < 0.0001$.

CR-01-64 to investigate the effects of opioid antagonists. Interestingly, naloxone did not block or reduce the analgesic action of CR-01-64 in our study (Fig. 3E). To our knowledge, these results are the first to show the nonopioid action of NT analogs acting at the NTS2 receptor.

The use of multimodal analgesia, which is defined as the administration of at least two analgesic drugs with different mechanisms of action, represents a successful strategy for the management of a wide range of pain conditions by minimizing the adverse effects associated with opioid treatment while improving pain control through the synergistic or additive actions of drug combinations [86,87]. Here, we evaluated whether a multimodal pharmacological approach combining NTS2 and opioid medications was potentially useful as a treatment option for the management of some pain conditions. For this purpose, morphine was administered intravenously at 1 mg/kg, alone or in combination with CR-01-64 (30 μg/kg; i.t.). As shown in Fig. 3E, morphine combined with CR-01-64 significantly increased the tail-flick latency compared to CR-01-64 or morphine alone, thus indicating that NT analogs are able to potentiate the analgesic effects of morphine. Accordingly, the combination of opioids with NT derivatives was found to increase analgesia through synergistic or additive effects [88–90].

3.2.2.2. CR-01-64 reduces formalin-evoked nociceptive behaviors. The antinociceptive effect of the macrocyclic compound CR-01-64 was then measured in the persistent inflammatory pain model induced by formalin by monitoring the paw licking, biting, shaking and lifting nociceptive behaviors induced by an intraplantar injection of diluted formalin (5%) into the right hind paw. Formalin-induced pain produced a typical biphasic behavioral response characterized by an early acute phase (0–9 min) and a sustained inflammatory phase (21–60 min) separated by a transient inactive interphase. Intrathecal injection of CR-01-64 dose-dependently reduced formalin-induced nociceptive behaviors in both the acute and inflammatory phases (Fig. 4A). Compared to saline-treated rats, the reduction in pain intensity score defined as the area under the curve (AUC) was effective even at the very low dose of 3 μg/kg, producing complete pain relief at 30 μg/kg (Fig. 4B). The median effective analgesic dose of CR-01-64 was estimated to be 7.1 μg/kg, similar to that obtained in the tail-flick acute pain paradigm (Fig. 4C). When focusing on the inflammatory phase, CR-01-64 was effective at reducing both spinal (lifting) and supraspinal (licking/biting/shaking) pain behaviors, while other NTS2-selective compounds, such as JMV-431 and levocabastine, only affected the spine-related lifting behaviors [47].

3.2.2.3. CR-01-64 alleviates mechanical hypersensitivity in a rat model of chronic inflammatory pain. We next investigated the analgesic effectiveness of CR-01-64 in a complete Freund's adjuvant (CFA)-induced chronic inflammatory pain model. Following a unilateral injection of CFA into the plantar surface of the rat hind paw, rats exhibited progressive swelling of the ipsilateral hind paw, accompanied by persistent hypersensitivity to nonpainful mechanical stimuli caused by a series of von Frey filaments. The paw withdrawal threshold was significantly reduced as early as day 3 post-CFA injection and was maintained at least until day 14 compared to sham animals (Fig. 5A). On days 7 and 14 post-CFA, the intrathecal injection of CR-01-64 at 60 μg/kg induced an increase in the paw withdrawal threshold, which lasted up to 60 min (Fig. 5B and C). Indeed, CR-01-64 exerted potent antiallodynic effects, inducing more than 80% pain relief, compared to saline-treated rats. To our knowledge, CR-01-64 is the first NT analog with selectivity for NTS2 reported to date that shows analgesic efficacy in the CFA model of chronic inflammatory joint pain.

3.2.3. Other NT-mediated physiological effects

NT is involved in the regulation of a number of other physiological functions. Among them, central or systemic administration of NT analogs has been shown to produce mild hypothermia and to exert neuroprotective effects on various neurological conditions, such as ischemic stroke and traumatic brain injury [40,91–94]. Peripherally, NT also regulates the gastrointestinal and cardiovascular systems, inducing changes in gastric and colonic motility and modulating blood pressure and myocardial contractility [12,13,38,39,95]. Importantly, preclinical

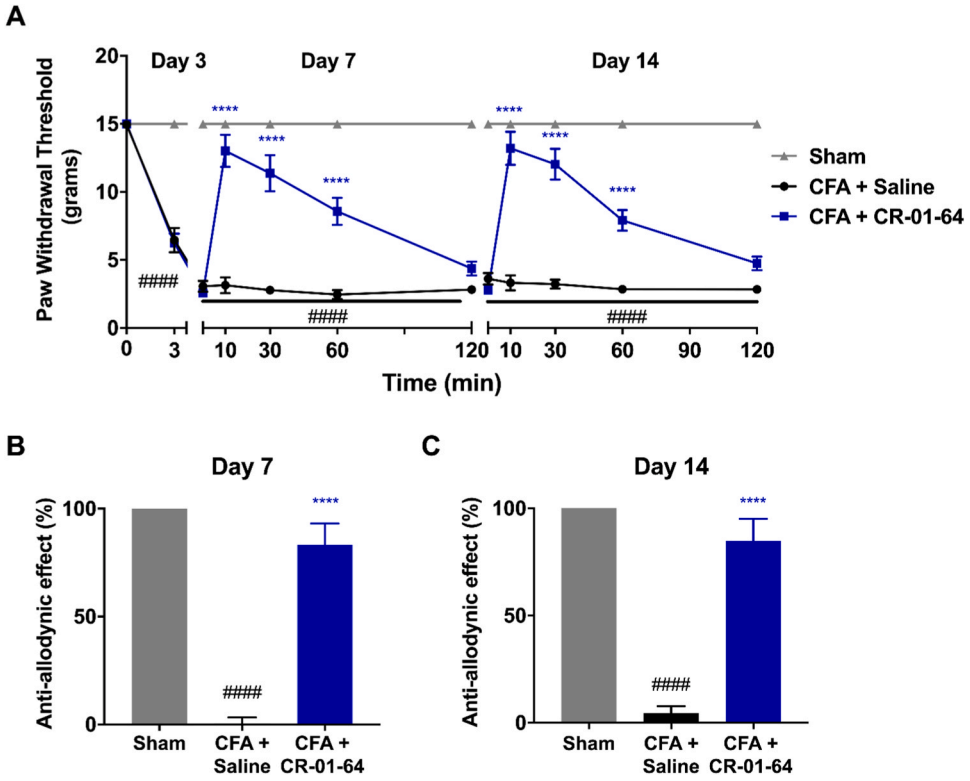

Fig. 5. Anti-allodynic effect of CR-01-64 on a chronic inflammatory pain model. (A) Mechanical anti-allodynic effects of CR-01-64 (60 μg/kg, i.t.) were determined at days 7 and 14 after the induction of inflammatory pain by complete Freund's adjuvant (CFA). The percent of anti-allodynic effect was determined at the maximal analgesic effect, 10 min post-injection, on day 7 (B) or 14 (C). The results are presented as the means ± SEM (N = 6/group). For the analysis of the time course of the effects on days 3, 7 and 14, comparisons between sham animals and CFA rats treated with saline (#) or between CFA rats receiving either saline or CR-01-64 (*) were performed using two-way analysis of variance for repeated measures followed by multiple comparisons using Dunnett's correction. For the % of anti-allodynic effect determined on days 7 and 14, comparisons between sham animals and CFA rats treated with saline (#) or CFA rats receiving either saline or CR-01-64 (*) were performed using one-way analysis of variance for repeated measures followed by multiple comparisons using Dunnett's correction. ****$p < 0.0001$ and ####$p < 0.0001$.

studies performed on NTS1-deficient mice or with the NTS1-selective antagonist SR48692 revealed that all of these physiological effects are exclusively associated with NTS1 activation [45,96–99]. We therefore decided to characterize the effects of CR-01-64 on the regulation of body temperature, blood pressure and ileum relaxation.

3.2.3.1. An analgesic dose of CR-01-64 does not induce hypothermia. The ability of CR-01-64 to modulate body temperature was then monitored at 10 min intervals for 60 min following i.t. administration and reported as the variation in temperature (Δ body temperature) from baseline before the injection. As shown in Fig. 6A, CR-01-64 did not produce hypothermia at the maximal analgesic dose tested (i.e., 60 μg/kg). In contrast, an injection of NT(8–13) at the same dose induced short-term hypothermia, while the NTS1-selective agonist PD149163 (h-LysΨ[CH2NH]Lys-Pro-Trp-Tle-Leu-OEt), an NT(8–13) analog that contains a reduced amine bond to improve its resistance to proteases, was responsible for a sustained decrease in body temperature, even at a lower dose of 30 μg/kg (Fig. 6A). Accordingly, nonselective macrocyclic analogs of NT(8–13) also induced a dose-dependent decrease in body temperature for over 1 h [50], while NTS2-selective ligands did not induce signs of hypothermia when injected centrally [45]. These results are also consistent with the presence of NTS1-immunopositive cell bodies and fibers in various nuclei of the hypothalamus known to control thermoregulation, such as the arcuate nucleus and the preoptic area [37].

3.2.3.2. CR-01-64 exerts moderate hypotensive effects at high doses. In addition to its hypothermic effects, intravenous (i.v.) or intracerebroventricular (i.c.v.) injection of NT analogs results in a significant decrease in blood pressure [38,100–102]. We thus evaluated the hypotensive action of CR-01-64 and NT(8–13) by monitoring the variation in arterial blood pressure (ΔMABP) using continuous intracarotid measurements. As observed in a previous study [103], an i.v. injection of NT (8–13) (0.1 mg/kg) induced a severe and sustained decrease in blood pressure characterized by a triphasic response (Fig. 6B). A short decrease of −25 mmHg occurred rapidly (first phase) before a swift return to basal levels (second phase) followed by a prolonged decrease to −50 mmHg (third phase). At a 10-fold lower dose (0.01 mg/kg; i.v.), NT (8–13) did not elicit the last sustained hypotensive phase. In comparison, an i.v. injection of CR-01-64 at the lowest dose of 0.01 mg/kg produced slight and transient hypotension lasting approximately two minutes, while a dose of 0.1 mg/kg induced moderate triphasic hypotension that was less than a similar dose of NT(8–13) and lasted up to 15 min (Fig. 6B). In the same experimental paradigm, nonselective

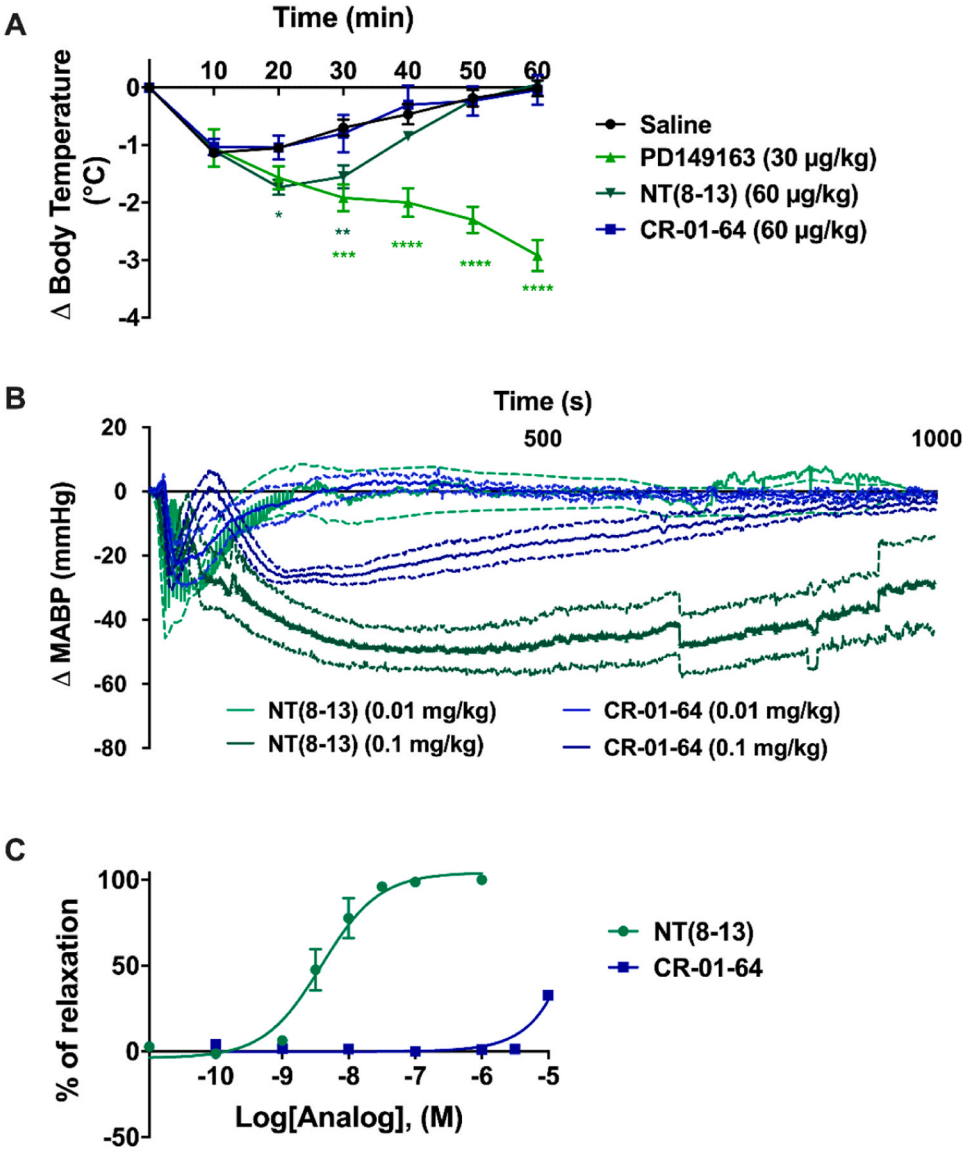

Fig. 6. Effects of CR-01-64 on body temperature, blood pressure, and smooth muscle contraction in Sprague-Dawley rats. (A) Variation in body temperature measured after the intrathecal injection of CR-01-64 and NT(8–13) at 60 μg/kg, PD149163 (NTS1-selective agonist) at 30 μg/kg or saline. (B) The change in mean arterial blood pressure (ΔMABP) recorded after the intravenous injection of NT (8–13) or CR-01-64 at 0.01 or 0.1 mg/kg to Sprague-Dawley rats. (C) Percent ileum relaxation monitored following an incubation with increasing concentrations of CR-01-64 or NT (8−13) ranging from 10^{-11} to 10^{-5} M. The results are presented as the means ± SEM (N = 6/group for body temperature measurements and N = 5/group for ΔMABP measurements). For body temperature, comparisons between groups treated with saline and PD149163 or CR-01-64 were performed using two-way analysis of variance for repeated measures followed by multiple comparisons using Dunnett's correction. Nonlinear regression analyses using three parameters were performed for % ileum relaxation. The NT(8–13) EC_{50} value was obtained from the resulting dose-response curve. *$p < 0.05$, **$p < 0.01$, ***$p < 0.001$, and ****$p < 0.0001$.

macrocyclic NT(8−13) analogs produced strong and persistent hypotension, similar to NT(8–13) [50]. The remaining hypotensive action of CR-01-64 is probably related to its ability to bind to NTS1, since the NTS2-selective compound NT79 ((NαMe)Arg-Arg-Pro-D-3,1-Nal-tLeu--Leu) does not lower blood pressure when injected intraperitoneally at a high dose of 5 mg/kg in freely moving rats [46]. Despite this moderate decrease in blood pressure, CR-01-64 offers a wider therapeutic window than nonselective NT analogs.

3.2.3.3. Ileum relaxation is not induced by CR-01-64. NT is a gastrointestinal peptide known to induce relaxation of colonic smooth muscles [39,95,104,105]. We thus investigated whether CR-01-64 was able to modulate the smooth muscle tone of the isolated rat ileum prestimulated with carbachol (Fig. 6C). Compared to NT(8–13), which produced strong relaxation of the carbachol-contracted strips in the organ bath with an EC_{50} of 3.9 nM, CR-01-64 was not effective at relaxing isolated segments of smooth muscles at concentrations of up to 1 μM. These results support the predominant role of NTS1 in mediating the relaxation of the ileum. Moreover, NT agonists fail to induce contractile responses of isolated ileal strips in mice deficient in NTS1 [96].

3.3. Pharmacokinetics of CR-01-64

3.3.1. Stability in plasma and cerebrospinal fluid exceeds 24 h

As a peptide, NT exhibits low oral bioavailability and low resistance to proteolytic degradation, which limits its clinical therapeutic use [106]. Its short half-life of approximately 2 min is due to rapid cleavage by three metalloendopeptidases (24.11, 24.15, and 24.16) at the peptide bonds Arg^8-Arg^9, Pro^{10}-Tyr^{11} and Tyr^{11}-Ile^{12} [107–110]. The metabolic stabilities of CR-01-64 and NT(8–13) were thus assessed in rat plasma and cerebrospinal fluid (CSF) at 37 °C for up to 24 h, and their degradation profiles were analyzed using UPLC-MS. As expected, rapid degradation of NT(8–13) was observed in plasma with a half-life of 2 min (Fig. 7A). Unlike blood, the stability of NT(8–13) in CSF was higher (half-life = 20 h), probably due to a lower proteolytic enzyme activity profile (Fig. 7B).

In both plasma and CSF, CR-01-64 exhibited excellent stability with a half-life of 24 h, indicating that macrocyclization limits peptide bond hydrolysis. Indeed, macrocyclization protects well-recognized degradation sites, notably Ile^{12}-Leu^{13}, Pro^{10}-Tyr^{11} and dibasic Arg^8-Arg^9 site amide bonds, which are readily hydrolyzed by enzymes, such as the angiotensin-converting enzyme and enkephalinases that are expressed at high levels in rat synaptic brain membranes [107–109]. In addition, the conformational restriction of the peptide backbone creates unfavorable folding, with presumably fewer beta-strand-like properties, thus preventing recognition by endopeptidases [111]. Therefore, CR-01-64 shows lower polarity and improved stability in plasma and CSF compared to NT(8–13).

3.3.2. Pharmacokinetic profile of CR-01-64

To our knowledge, the plasma and cerebrospinal fluid (CSF) pharmacokinetics (PK) of NTS2 compounds have never been evaluated and are therefore of interest in the development of new analgesics. Optimizing the ADME properties of a molecule is indeed a challenging part of the whole drug discovery process since the PK profile has a major effect on the likelihood of a drug's success and will also help determine the appropriate route of administration in a clinical setting. Here, we subsequently determined the PK profiles of CR-01-64 by collecting plasma and CSF samples at various time points following i.v. and i.t. administration, respectively.

The time course of plasma concentrations following an i.v. injection of CR-01-64 at 0.2 mg/kg, as well as in CSF after an i.t. injection of 60 μg/kg are shown in Fig. 8A and B. The associated PK parameters are shown in Tables 1 and 2. The plasma PK of CR-01-64, which were analyzed using a two-compartmental model, displayed rapid elimination with a short elimination half-life and high elimination rate constant and clearance. CR-01-64 also exhibited high distribution volumes. Exposure to CR-01-64 and the mean residence time were low. Indeed, plasma PK revealed that CR-01-64 was rapidly removed from plasma with first-order elimination kinetics ($t_{1/2}\beta$ = 44.7 min and Cl = 0.38 L/min/kg), and was CR-01-64 broadly distributed (V_1 = 2.63 L/kg and V_{SS} = 9.44 L/kg), indicating tissue diffusion. We hypothesize that renal excretion probably contributes to its rapid elimination from plasma, given the peptidic nature of CR-01-64.

Likewise, the PK of CR-01-64 in CSF, which were analyzed using noncompartmental analysis, exhibited rapid elimination with a short elimination half-life and high elimination rate constant and clearance. The macrocycle was broadly distributed with a large volume of distribution. Its exposure and mean residence time were low. The PK analysis in CSF indicated a delayed C_{max} at 90 min, as CR-01-64 was injected intrathecally between the L5-L6 intervertebral space and collected above in the cisterna magna. It also exhibited rapid clearance from the CSF and a high distribution ($t_{1/2}\lambda z$ = 55.49 min and V_Z/F = 0.26 L/kg), indicating tissue diffusion. Interestingly, CSF concentrations of CR-01-64 represented less than 1% of the administered dose (60 μg/kg), consistent with its tissue diffusion. CR-01-64 therefore appears to exhibit a favorable PK profile in CSF, which may govern its long-lasting analgesic effects. Together, these results indicate that the macrocyclization of NT analogs is a successful strategy to develop stable compounds and to improve the ADME properties.

4. Conclusions

There is a very high need for improving the management of acute and persistent pain since its pharmacotherapy remains often limited. To support the development of analgesics, more predictive assessments of target engagement and response to drug treatment are needed. For instance, the incorporation of translational tools, such as validated pharmacodynamic (PD) biomarkers can provide important information

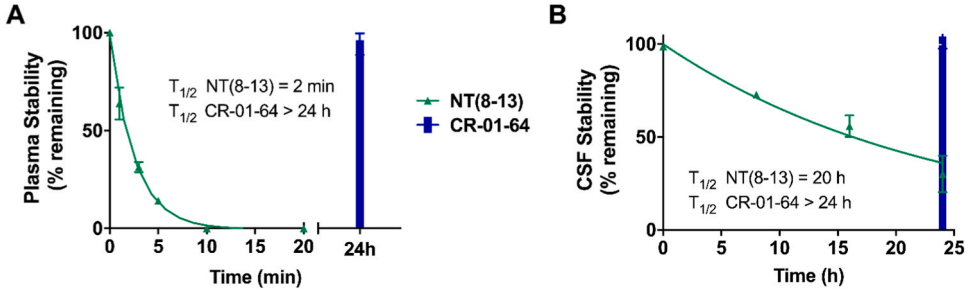

Fig. 7. Metabolic stability of CR-01-64 in rat biological fluids. In vitro stability of NT(8–13) and CR-01-64 in rat plasma (A) and cerebrospinal fluid (CSF) (B). The half-life ($t_{1/2}$) was calculated as the disappearance of half of the compound (% remaining) determined using UPLC-MS. Error bars represent the means ± SEM of at least three separate experiments using each compound.

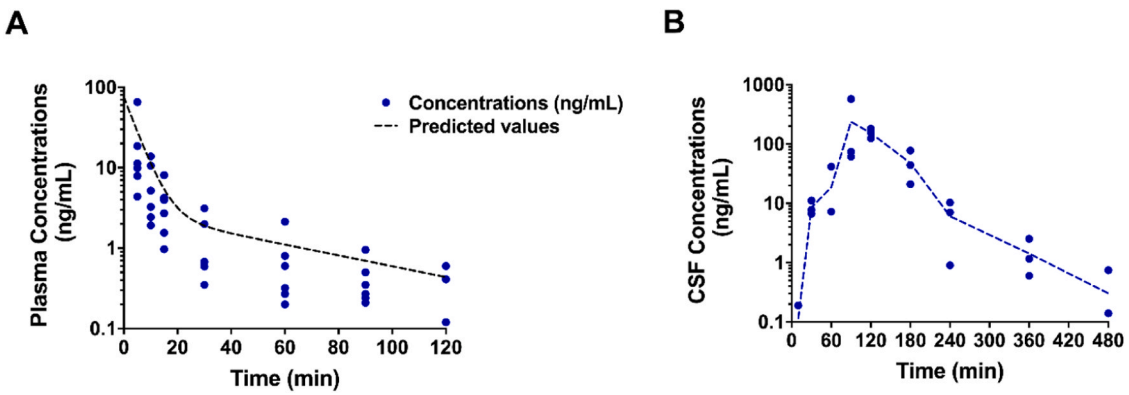

Fig. 8. Pharmacokinetic profile of CR-01-64 in rat biological fluids. (A) Plasma CR-01-64 concentration-time profiles following an intravenous injection of 0.2 mg/kg CR-01-64 in SD rats show the observed (blue circle) and predicted (black dashed line) concentrations using a two-compartment model (N = 6). (B) CSF CR-01-64 concentration-time profiles following an intrathecal injection of 60 μg/kg CR-01-64 in SD rats show the observed (blue circle) and mean (black dashed line) concentrations (N = 27 rats). For interpretation of the references to color in this figure legend, the reader is referred to the web version of this article.

Table 1
Plasma pharmacokinetic parameters following an intravenous injection of 0.2 mg/kg CR-01-64 in Sprague-Dawley rats. Parameters were determined using a two-compartmental model (N = 6).

Parameters	Units	Plasma	
		Estimation	CV (%)
C_0	ng/mL	75.97	49.81
V_1	L/kg	2.63	49.86
k_{10}	min^{-1}	0.14	32.32
k_{12}	min^{-1}	0.06	29.67
k_{21}	min^{-1}	0.02	32.10
V_{SS}	L/kg	9.44	45.18
Cl	L/kg/min	0.38	19.89
α	min^{-1}	0.21	28.3
β	min^{-1}	0.016	29.5
$t_{1/2}α$	min	3.23	28.2
$t_{1/2}β$	min	44.7	29.5
MRT	min	25.12	30.27
AUC_{inf}	μg min/L	532.17	19.87

C0, initial plasma concentration; V1, central volume of distribution; k10, elimination rate constant; k12 and k21, transfer rate constants between central and peripheral compartments; VSS, volume of distribution at the steady state; Cl, total clearance; α, distribution rate constant, β, elimination rate constant, t1/2α, distribution half-life, t1/2β, elimination half-life; MRT, mean residence time; AUC_{inf}, area under the concentration-time curve. Values are presented as the means ± SD.

Table 2
CSF pharmacokinetic parameters following an intrathecal injection of 60 μg/kg CR-01-64 in Sprague-Dawley rats. Parameters were determined using a non-compartmental analysis (N = 27 rats).

Parameters	Units	CSF
		Estimation
T_{max}	min	90
C_{max}	ng/mL	236,310
λz	min^{-1}	0.01
V_Z/F	L/kg	0.26
Cl_Z/F	L/kg/min	0.003
$t_{1/2}$ λz	min	55.49
MRT	min	121.62
AUC_{last}	μg min/L	18,363

C_{max}, peak plasma concentration; T_{max}, time to achieve Cmax; λz, elimination rate constant; VZ/F, volume of distribution; Cl_Z/F, total clearance; $t_{1/2}$ λz, terminal elimination half-life; MRT, mean residence time; AUC_{last}, area under the concentration-time curve. Values are presented as the means ± SD.

about the pharmacological effects of a drug on its target, prove its efficacy throughout clinical phases and facilitate regulatory approval [112]. Unfortunately, unlike the field of oncology, which has been transformed by the use of biomarkers, to our knowledge, such biomarkers do not yet exist in the field of chronic pain [113,114]. Monitoring of blood or CSF PD biomarkers that rise or fall in response to drug treatment therefore has the potential to facilitate the assessment of the efficacy and safety issues of non-addictive pain therapeutics as well as to reduce attrition and high-failure rate in the development of analgesics [115].

The need for safe and effective alternatives to opioids has never been greater than during the current opioid epidemic. While opioids are recognized as the most effective pain-relieving drugs, the use of non-opioid analgesics and opioid-sparing multimodal therapy has the potential to limit the adverse effects of opioids by reducing the dose used. Importantly, this alternative strategy also provides an approach to mitigate the recognized dangers associated with opioid misuse and abuse. Regarding its analgesic action, CR-01-64 produces potent and effective antinociceptive responses to different sensory modalities (e.g., thermal, chemical and mechanical stimuli) in various models of acute, persistent, and chronic pain. Importantly, the analgesic effect of CR-01-64 does not appear to depend on the endogenous opioid system, since the administration of the opioid antagonist naloxone is not effective at reversing NT-induced analgesia. By activating a different mechanism of action, CR-01-64 combined with morphine further improves pain relief at lower doses of morphine than morphine alone. Overall, these results highlight the potential use of NTS2 as nonopioid analgesics or in a multimodal regimen with morphine to achieve more effective analgesia with reduced adverse effects.

Funding

This work was supported by funding from the Canadian Institutes of Health Research (FDN-148413 to P.S.), the Natural Sciences and Engineering Research Council of Canada and the Canadian Foundation for Innovation. P.S. is the holder of Canada Research Chair Tier 1 in the Neurophysiopharmacology of Chronic Pain and a member of the FRQS-funded Québec Pain Research Network. E.M. is a member of the FRQNT-funded Proteo and the FRQS-funded Québec Network for Drug Research networks. M.C.'s Ph.D. is funded by the FRQS. M.D. is a recipient of a fellowship from the Centre de Recherche du CHUS.

Dedication

In memory of our close colleague, best friend and research director, Professor Éric Marsault, who passed away far too early.

CRediT authorship contribution statement

Magali Chartier: Investigation, Formal analysis, Writing - original draft, Visualization. **Michael Desgagné:** Investigation, Methodology, Validation, Writing - original draft, Visualization. **Marc Sousbie:** Investigation. **Charles Rumsby:** Investigation. **Lucie Chevillard:** Formal analysis. Léa Théroux: Investigation. **Lounès Haroune:** Investigation, Methodology, Formal analysis. **Jérôme Côté:** Investigation, Formal analysis, Visualization,d Writing - review & editing. **Jean-Michel Longpré:** Formal analysis, Resources, Writing - review & editing. **Pierre-Luc Boudreault:** Supervision, Project administration. **Éric Marsault:** Conceptualization, Supervision, Project administration, Writing - review & editing, Funding acquisition. **Philippe Sarret:** Conceptualization, Supervision, Project administration, Writing - review & editing, Funding acquisition.

Declaration of Competing Interest

The authors declare that they have no known competing financial interests or personal relationships that have, or could be perceived to have, influenced the work reported in this article.

References

[1] D.S. Goldberg, S.J. McGee, Pain as a global public health priority, BMC Public Health 11 (2011) 770.
[2] C.J. Woolf, Capturing novel non-opioid pain targets, Biol. Psychiatry 87 (1) (2020) 74–81.
[3] D.E. Moulin, A.J. Clark, M. Speechley, P.K. Morley-Forster, Chronic pain in Canada—prevalence, treatment, impact and the role of opioid analgesia, Pain Res. Manag. 7 (4) (2002) 179–184.
[4] M.J. Perez de Vega, A. Ferrer-Montiel, R. Gonzalez-Muniz, Recent progress in non-opioid analgesic peptides, Arch. Biochem. Biophys. 660 (2018) 36–52.
[5] F. St-Gelais, C. Jomphe, L.E. Trudeau, The role of neurotensin in central nervous system pathophysiology: what is the evidence? J. Psychiatry Neurosci. 31 (4) (2006) 229–245.
[6] K. Liu, H. Khan, X. Geng, J. Zhang, Y. Ding, Pharmacological hypothermia: a potential for future stroke therapy? Neurol. Res. 38 (6) (2016) 478–490.
[7] L.E. Schroeder, G.M. Leinninger, Role of central neurotensin in regulating feeding: implications for the development and treatment of body weight disorders, Biochim. Biophys. Acta Mol. Basis Dis. 1864 (3) (2018) 900–916.
[8] P.R. Dobner, Neurotensin and pain modulation, Peptides 27 (10) (2006) 2405–2414.
[9] Y.-P. Feng, J. Wang, Y.-L. Dong, Y.-Y. Wang, Y.-Q. Li, The roles of neurotensin and its analogues in pain, Curr. Pharm. Des. 21 (7) (2015) 840–848.
[10] S. Geisler, A. Berod, D.S. Zahm, W. Rostene, Brain neurotensin, psychostimulants, and stress–emphasis on neuroanatomical substrates, Peptides 27 (10) (2006) 2364–2384.
[11] M. Boules, Z. Li, K. Smith, P. Fredrickson, E. Richelson, Diverse roles of neurotensin agonists in the central nervous system, Front. Endocrinol. 4 (2013) 436.
[12] O.E. Osadchii, Emerging role of neurotensin in regulation of the cardiovascular system, Eur. J. Pharmacol. 762 (2015) 184–192.
[13] D. Zhao, C. Pothoulakis, Effects of NT on gastrointestinal motility and secretion, and role in intestinal inflammation, Peptides 27 (10) (2006) 2434–2444.
[14] B.V. Clineschmidt, J.C. McGuffin, P.B. Bunting, Neurotensin: antinocisponsive action in rodents, Eur. J. Pharmacol. 54 (1979) 129–139.
[15] S. Sarhan, J.M. Hitchcock, C.A. Grauffel, J.G. Wettstein, Comparative antipsychotic profiles of neurotensin and a related systemically active peptide agonist, Peptides 18 (8) (1997) 1223–1227.
[16] B.V. Clineschmidt, G.E. Martin, D.F. Veber, Antinocisponsive effects of neurotensin and neurotensin-related peptides, Ann. N. Y. Acad. Sci. 400 (1982) 283–306.
[17] P. Bredeloux, J. Costentin, I. Dubuc, Interactions between NTS2 neurotensin and opioid receptors on two nociceptive responses assessed on the hot plate test in mice, Behav. Brain Res. 175 (2) (2006) 399–407.
[18] M.M. Behbehani, A. Pert, A mechanism for the analgesic effect of neurotensin as revealed by behavioral and electrophysiological techniques, Brain Res. 324 (1) (1984) 35–42.
[19] B.V. Clineschmidt, J.C. McGuffin, Neurotensin administered intracisternally inhibits responsiveness of mice to noxious stimuli, Eur. J. Pharm. 46 (4) (1977) 395–396.
[20] A. Coquerel, I. Dubuc, P. Kitaegi, J. Costentin, Potentiation by thiorphan and bestatin of the naloxone-insensitive analgesic effects of neurotensin and neuromedin n, Neurochem. Int. 12 (3) (1988) 361–366.
[21] A.J. Osbahr 3rd, C.B. Nemeroff, D. Luttinger, G.A. Mason, A.J. Prange Jr., Neurotensin-induced antinociception in mice: antagonism by thyrotropin-releasing hormone, J. Pharm. Exp. Ther. 217 (3) (1981) 645–651.
[22] D.J. Wustrow, M.D. Davis, H.C. Akunne, A.E. Corbin, J.N. Wiley, L.D. Wise, T. G. Heffner, Reduced amide bond neurotensin 8-13 mimetics with potent in vivo activity, Bioorg. Med. Chem. Lett. 5 (1995) 997–1002.
[23] E. Eiselt, S. Gonzalez, C. Martin, M. Chartier, C. Betti, J.-M. Longpré, F. Cavelier, D. Tourwé, L. Gendron, S. Ballet, P. Sarret, Neurotensin analogues containing cyclic surrogates of tyrosine at position 11 improve NTS2 selectivity leading to analgesia without hypotension and hypothermia, ACS Chem. Neurosci. 10 (11) (2019) 4535–4544.
[24] C.B. Nemeroff, A.J. Osbahr, P.J. Manberg, G.N. Ervin, A.J. Prange, Alterations in nociception and body temperature after intracisternal administration of neurotensin, beta-endorphin, other endogenous peptides, and morphine, Proc. Natl. Acad. Sci. USA 76 (10) (1979) 5368–5371.
[25] N.R. al-Rodhan, E. Richelson, J.A. Gilbert, D.J. McCormick, K.S. Kanba, M. A. Pfenning, A. Nelson, E.W. Larson, T.L. Yaksh, Structure-antinociceptive activity of neurotensin and some novel analogues in the periaqueductal gray region of the brainstem, Brain Res 557 (1–2) (1991) 227–235.
[26] P. Tétreault, N. Beaudet, A. Perron, K. Belleville, A. René, F. Cavelier, J. Martinez, T. Stroh, A.M. Jacobi, S.D. Rose, M.A. Behlke, P. Sarret, Spinal NTS2 receptor activation reverses signs of neuropathic pain, FASEB J.: Off. Publ. Fed. Am. Soc. Exp. Biol. 27 (9) (2013) 3741–3752.
[27] P. Kleczkowska, A.W. Lipkowski, Neurotensin and neurotensin receptors: characteristic, structure-activity relationship and pain modulation—a review, Eur. J. Pharmacol. 716 (1–3) (2013) 54–60.
[28] P. Sarret, F. Cavelier, Neurotensin and Its Receptors, Reference Module in Neuroscience and Biobehavioral Psychology, Elsevier, 2018, pp. 1–17.
[29] M.L. Asselin, I. Dubuc, A. Coquerel, J. Costentin, Localization of neurotensin NTS2 receptors in rat brain, using [3H]Levocabastine, Neuroreport 12 (5) (2001) 1087–1091.
[30] H. Boudin, D. Pélaprat, W. Rostène, A. Beaudet, Cellular distribution of neurotensin receptors in rat brain: immunohistochemical study using an antipeptide antibody against the cloned high affinity receptor, J. Comp. Neurol. 373 (1) (1996) 76–89.
[31] A.V. Buhler, J. Choi, H.K. Proudfit, G.F. Gebhart, Neurotensin activation of the NTR1 on spinally-projecting serotonergic neurons in the rostral ventromedial medulla is antinociceptive, Pain 114 (1–2) (2005) 285–294.
[32] G. Roussy, M.-A. Dansereau, L. Doré-Savard, K. Belleville, N. Beaudet, E. Richelson, P. Sarret, Spinal NTS1 receptors regulate nociceptive signaling in a rat formalin tonic pain model, J. Neurochem. 105 (4) (2008) 1100–1114.
[33] P. Sarret, M.J. Esdaile, A. Perron, J. Martinez, T. Stroh, A. Beaudet, Potent spinal analgesia elicited through stimulation of NTS2 neurotensin receptors, J. Neurosci.: Off. J. Soc. Neurosci. 25 (36) (2005) 8188–8196.
[34] P. Sarret, A. Perron, T. Stroh, A. Beaudet, Immunohistochemical distribution of NTS2 neurotensin receptors in the rat central nervous system, J. Comp. Neurol. 461 (4) (2003) 520–538.
[35] P. Sarret, A. Beaudet, Neurotensin receptors in the central nervous system, in: R. Quirion, A. Björklund, T. Hökfelt (Eds.), Handbook of Chemical Neuroanatomy, Peptide Receptors, Pt II, Elsevier, Amsterdam, 2002, pp. 323–400.
[36] P. Sarret, A. Beaudet, J.P. Vincent, J. Mazella, Regional and cellular distribution of low affinity neurotensin receptor mRNA in adult and developing mouse brain, J. Comp. Neurol. 394 (3) (1998) 344–356.
[37] A. Fassio, G. Evans, R. Grisshammer, J.P. Bolam, M. Mimmack, P.C. Emson, Distribution of the neurotensin receptor NTS1 in the rat CNS studied using an amino-terminal directed antibody, Neuropharmacology 39 (8) (2000) 1430–1442.
[38] W.E. Fantegrossi, M.C.H. Ko, J.H. Woods, E. Richelson, Antinociceptive, hypothermic, hypotensive, and reinforcing effects of a novel neurotensin receptor agonist, NT69L, in rhesus monkeys, Pharmacol. Biochem. Behav. 80 (2) (2005) 341–349.
[39] S. Pellissier, O. Eribon, J. Chabert, D. Gully, M. Roche, Peripheral neurotensin participates in the modulation of pre- and postprandial intestinal motility in rats, Neuropeptides 30 (5) (1996) 412–419.
[40] S. Previti, M. Vivancos, E. Remond, S. Beaulieu, J.M. Longpre, S. Ballet, P. Sarret, F. Cavelier, Insightful backbone modifications preventing proteolytic degradation of neurotensin analogs improve NTS1-induced protective hypothermia, Front. Chem. 8 (2020) 406.
[41] C. Granier, J. van Rietschoten, P. Kitabgi, C. Poustis, P. Freychet, Synthesis and characterization of neurotensin analogues for structure/activity relationship studies. Acetyl-neurotensin-(8–13) is the shortest analogue with full binding and pharmacological activities, Eur. J. Biochem. 124 (1) (1982) 117–124.
[42] A.V. Buhler, H.K. Proudfit, G.F. Gebhart, Neurotensin-produced antinociception in the rostral ventromedial medulla is partially mediated by spinal cord norepinephrine, Pain 135 (3) (2008) 280–290.
[43] A. Guillemette, M.A. Dansereau, N. Beaudet, E. Richelson, P. Sarret, Intrathecal administration of NTS1 agonists reverses nociceptive behaviors in a rat model of neuropathic pain, Eur. J. Pain 16 (4) (2012) 473–484.
[44] K.E. Smith, M. Boules, K. Williams, E. Richelson, NTS1 and NTS2 mediate analgesia following neurotensin analog treatment in a mouse model for visceral pain, Behav. Brain Res. 232 (1) (2012) 93–97.
[45] I. Dubuc, P. Sarret, C. Labbé-Jullié, J.M. Botto, E. Honoré, E. Bourdel, J. Martinez, J. Costentin, J.P. Vincent, P. Kitabgi, J. Mazella, Identification of the receptor subtype involved in the analgesic effect of neurotensin, J. Neurosci.: Off. J. Soc. Neurosci. 19 (1) (1999) 503–510.
[46] M. Boules, Y. Liang, S. Briody, T. Miura, I. Fauq, A. Oliveros, M. Wilson, S. Khaniyev, K. Williams, Z. Li, Y. Qi, M. Katovich, E. Richelson, NT79: a novel

neurotensin analog with selective behavioral effects, Brain Res. 1308 (2010) 35–46.
[47] G. Roussy, M.-A. Dansereau, S. Baudisson, F. Ezzoubaa, K. Belleville, N. Beaudet, J. Martinez, E. Richelson, P. Sarret, Evidence for a role of NTS2 receptors in the modulation of tonic pain sensitivity, Mol. Pain 5 (2009) 38.
[48] A.P. Davenport, C.C.G. Scully, C. de Graaf, A.J.H. Brown, J.J. Maguire, Advances in therapeutic peptides targeting G protein-coupled receptors, Nat. Rev. Drug Discov. 19 (6) (2020) 389–413.
[49] M. Sousbie, É. Besserer-Offroy, R.L. Brouillette, J.-M. Longpré, R. Leduc, P. Sarret, É. Marsault, In search of the optimal macrocyclization site for neurotensin, ACS Med. Chem. Lett. 9 (3) (2018) 227–232.
[50] M. Sousbie, M. Vivancos, R.L. Brouillette, É. Besserer-Offroy, J.-M. Longpré, R. Leduc, P. Sarret, É. Marsault, Structural optimization and characterization of potent analgesic macrocyclic analogues of neurotensin (8-13), J. Med. Chem. 61 (16) (2018) 7103–7115.
[51] E. Marsault, M.L. Peterson. Practical Medicinal Chemistry with Macrocycles: Design, Synthesis, and Case Studies, first ed., John Wiley & Sons,, 2017.
[52] E. Marsault, M.L. Peterson, Macrocycles are great cycles: applications, opportunities, and challenges of synthetic macrocycles in drug discovery, J. Med Chem. 54 (7) (2011) 1961–2004.
[53] J. Mallinson, I. Collins, Macrocycles in new drug discovery, Future Med. Chem. 4 (11) (2012) 1409–1438.
[54] P. Bredeloux, F. Cavelier, I. Dubuc, B. Vivet, J. Costentin, J. Martinez, Synthesis and biological effects of c(Lys-Lys-Pro-Tyr-Ile-Leu-Lys-Lys-Pro-Tyr-Ile-Leu) (JMV2012), a new analogue of neurotensin that crosses the blood-brain barrier, J. Med. Chem. 51 (6) (2008) 1610–1616.
[55] J. Einsiedel, C. Held, M.P. Hervet, T. M, H. N, G. H, P, Discovery of highly potent and neurotensin receptor 2 selective neurotensin mimetics, J. Med. Chem. 54 (2011) 2915–2923.
[56] R. Fanelli, N. Floquet, É. Besserer-Offroy, B. Delort, M. Vivancos, J.M. Longpré, P. Renault, J. Martinez, P. Sarret, F. Cavelier, Use of molecular modeling to design selective NTS2 neurotensin analogues, J. Med. Chem. 60 (2017) 3303–3313.
[57] C. Schaab, R.C. Kling, J. Einsiedel, H. Hübner, T. Clark, D. Seebach, P. Gmeiner, Structure-based evolution of subtype-selective neurotensin receptor ligands, ChemistryOpen 3 (5) (2014) 206–218.
[58] C. Held, M. Plomer, H. Hubner, J. Meltretter, M. Pischetsrieder, P. Gmeiner, Development of a metabolically stable neurotensin receptor 2 (NTS2) ligand, ChemMedChem 8 (1) (2013) 75–81.
[59] G. Pratsch, J.F. Unfried, J. Einsiedel, M. Plomer, H. Hubner, P. Gmeiner, M. R. Heinrich, Radical arylation of tyrosine and its application in the synthesis of a highly selective neurotensin receptor 2 ligand, Org. Biomol. Chem. 9 (10) (2011) 3746–3752.
[60] N.A. Simeth, M. Bause, M. Dobmeier, R.C. Kling, D. Lachmann, H. Hubner, J. Einsiedel, P. Gmeiner, B. Konig, NTS2-selective neurotensin mimetics with tetrahydrofuran amino acids, Bioorg. Med. Chem. 25 (1) (2017) 350–359.
[61] F. Richard, S. Barroso, J. Martinez, C. Labbe-Jullie, P. Kitabgi, Agonism, inverse agonism, and neutral antagonism at the constitutively active human neurotensin receptor 2, Mol. Pharm. 60 (6) (2001) 1392–1398.
[62] Y. Cheng, W.H. Prusoff, Relationship between the inhibition constant (K1) and the concentration of inhibitor which causes 50 per cent inhibition (I50) of an enzymatic reaction, Biochem. Pharm. 22 (1973) 3099–3108.
[63] C. Kilkenny, W.J. Browne, I.C. Cuthill, M. Emerson, D.G. Altman, Improving bioscience research reporting: the ARRIVE guidelines for reporting animal research, PLOS Biol. 8 (6) (2010), 1000412.
[64] C.F. Kallina, J.W. Grau, Tail-flick test. I: impact of a suprathreshold exposure to radiant heat on pain reactivity in rats, Physiol. Behav. 58 (1) (1995) 161–168.
[65] A. Tjølsen, O.G. Berge, S. Hunskaar, J.H. Rosland, K. Hole, The formalin test: an evaluation of the method, Pain 51 (1) (1992) 5–17.
[66] T.J. Coderre, The role of excitatory amino acid receptors and intracellular messengers in persistent nociception after tissue injury in rats, Mol. Neurobiol. 7 (3–4) (1993) 229–246.
[67] D. Dubuisson, S.G. Dennis, The formalin test: a quantitative study of the analgesic effects of morphine, meperidine, and brain stem stimulation in rats and cats, Pain 4 (2) (1977) 161–174.
[68] S.R. Chaplan, F.W. Bach, J.W. Pogrel, J.M. Chung, T.L. Yaksh, Quantitative assessment of tactile allodynia in the rat paw, J. Neurosci. Methods 53 (1) (1994) 55–63.
[69] R. Nirogi, V. Kandikere, K. Mudigonda, G. Bhyrapuneni, N. Muddana, R. Saralaya, V. Benade, A simple and rapid method to collect the cerebrospinal fluid of rats and its application for the assessment of drug penetration into the central nervous system, J. Neurosci. Methods 178 (1) (2009) 116–119.
[70] M.J. Curtis, S. Alexander, G. Cirino, J.R. Docherty, C.H. George, M.A. Giembycz, D. Hoyer, P.A. Insel, A.A. Izzo, Y. Ji, D.J. MacEwan, C.G. Sobey, S.C. Stanford, M. M. Teixeira, S. Wonnacott, A. Ahluwalia, Experimental design and analysis and their reporting II: updated and simplified guidance for authors and peer reviewers, Br. J. Pharmacol. 175 (7) (2018) 987–993.
[71] F. Giordanetto, J. Kihlberg, Macrocyclic drugs and clinical candidates: what can medicinal chemists learn from their properties? J. Med. Chem. 57 (2) (2014) 278–295.
[72] X. Jing, K. Jin, A gold mine for drug discovery: strategies to develop cyclic peptides into therapies, Med. Res. Rev. 40 (2) (2020) 753–810.
[73] A. Zorzi, K. Deyle, C. Heinis, Cyclic peptide therapeutics: past, present and future, Curr. Opin. Chem. Biol. 38 (2017) 24–29.
[74] S. Stotani, F. Giordanetto, Overview of macrocycles in clinical development and clinically used, in: E. Marsault, M.L. Peterson (Eds.), Practical Medicinal Chemistry with Macrocycles: Design, Synthesis, and Case Studies, John Wiley & Sons, 2017, pp. 411–499.
[75] A.M. Sefler, J.X. He, T.K. Sawyer, K.E. Holub, D.O. Omecinsky, M.D. Reily, V. Thanabal, H.C. Akunne, W.L. Cody, Design and structure-activity relationships of C-terminal cyclic neurotensin fragment analogues, J. Med. Chem. 38 (2) (1995) 249–257.
[76] H.C. Akunne, S. Darling, K. Zoski, A.M. Sefler, J.X. He, T.K. Sawyer, T.A. Pugsley, W.L. Cody, Functional activity of new C-terminal cyclic-neurotensin fragment analogs, Neuropeptides 30 (3) (1996) 213–218.
[77] F.M. Van Kemmel, I. Dubuc, E. Bourdel, J.A. Fehrentz, J. Martinez, J. Costentin, A. C-terminal, cyclic 8-13 neurotensin fragment analog appears less exposed to neprilysin when it crosses the blood-brain barrier than the cerebrospinal fluid-brain barrier in mice, Neurosci. Lett. 217 (1) (1996) 58–60.
[78] J.Tt Lundquist, T.A. Dix, Preparation and receptor binding affinities of cyclic C-terminal neurotensin (8-13) and (9-13) analogues, Bioorg. Med. Chem. Lett. 9 (17) (1999) 2579–2582.
[79] J.B. Thomas, M. Vivancos, A.M. Giddings, R.W. Wiethe, K.R. Warner, A. Murza, E. Besserer-Offroy, J.M. Longpre, S.P. Runyon, A.M. Decker, B.P. Gilmour, P. Sarret, Identification of 2-({[1-(4-Fluorophenyl)-5-(2-methoxyphenyl)-1H-pyrazol-3-yl]carbonyl}amino)tricyc lo[3.3.1.13,7]decane-2-carboxylic acid (NTRC-844) as a selective antagonist for the rat neurotensin receptor type 2, ACS Chem. Neurosci. 7 (9) (2016) 1225–1231.
[80] D.G. Udugamasooriya, M.R. Spaller, Conformational constraint in protein ligand design and the inconsistency of binding entropy, Biopolymers 89 (8) (2008) 653–667.
[81] P. Kleczkowska, A.W. Lipkowski, D. Tourwe, S. Ballet, Hybrid opioid/non-opioid ligands in pain research, Curr. Pharm. Des. 19 (42) (2013) 7435–7450.
[82] B.M. McMahon, J.A. Stewart, J. Jackson, A. Fauq, D.J. McCormick, E. Richelson, Intraperitoneal injection of antisense peptide nucleic acids targeted to the mu receptor decreases response to morphine and receptor protein levels in rat brain, Brain Res 904 (2) (2001) 345–349.
[83] G. Roussy, H. Beaudry, M. Lafrance, K. Belleville, N. Beaudet, K. Wada, L. Gendron, P. Sarret, Altered morphine-induced analgesia in neurotensin type 1 receptor null mice, Neuroscience 170 (4) (2010) 1286–1294.
[84] S.A. Tershner, F.J. Helmstetter, Antinociception produced by mu opioid receptor activation in the amygdala is partly dependent on activation of mu opioid and neurotensin receptors in the ventral periaqueductal gray, Brain Res. 865 (1) (2000) 17–26.
[85] C.O. Stiller, H. Gustafsson, K. Fried, E. Brodin, Opioid-induced release of neurotensin in the periaqueductal gray matter of freely moving rats, Brain Res 774 (1–2) (1997) 149–158.
[86] I. Gilron, T.S. Jensen, A.H. Dickenson, Combination pharmacotherapy for management of chronic pain: from bench to bedside, Lancet Neurol. 12 (11) (2013) 1084–1095.
[87] J.X. Li, Combining opioids and non-opioids for pain management: current status, Neuropharmacology 158 (2019), 107619.
[88] E. Eiselt, J. Cote, J.M. Longpre, V. Blais, P. Sarret, L. Gendron, The combination of opioid and neurotensin receptor agonists improves their analgesic/adverse effect ratio, Eur. J. Pharm. 848 (2019) 80–87.
[89] M. Boules, A. Shaw, Y. Liang, D. Barbut, E. Richelson, NT69L, a novel analgesic, shows synergy with morphine, Brain Res. 1294 (2009) 22–28.
[90] M. Boules, H. Johnston, J. Tozy, K. Smith, Z. Li, E. Richelson, Analgesic synergy of neurotensin receptor subtype 2 agonist NT79 and morphine, Behav. Pharm. 22 (5–6) (2011) 573–581.
[91] G. Bissette, D. Luttinger, G.A. Mason, D.E. Hernandez, P.T. Loosen, Neurotensin and thermoregulation, Ann. N. Y. Acad. Sci. 400 (1982) 268–282.
[92] X. Gu, Z.Z. Wei, A. Espinera, J.H. Lee, X. Ji, L. Wei, T.A. Dix, S.P. Yu, Pharmacologically induced hypothermia attenuates traumatic brain injury in neonatal rats, Exp. Neurol. 267 (2015) 135–142.
[93] Y. Zhao, Z.Z. Wei, J.H. Lee, X. Gu, J. Sun, T.A. Dix, L. Wei, S.P. Yu, Pharmacological hypothermia induced neurovascular protection after severe stroke of transient middle cerebral artery occlusion in mice, Exp. Neurol. 325 (2020), 113133.
[94] K.E. Choi, C.L. Hall, J.M. Sun, L. Wei, O. Mohamad, T.A. Dix, S.P. Yu, A novel stroke therapy of pharmacologically induced hypothermia after focal cerebral ischemia in mice, FASEB J. 26 (7) (2012) 2799–2810.
[95] F. Mulè, R. Serio, Mode and mechanism of neurotensin action in rat proximal colon, Eur. J. Pharmacol. 319 (2–3) (1997) 269–272.
[96] D.J. Pettibone, J.F. Hess, P.J. Hey, M.A. Jacobson, M. Leviten, E.V. Lis, P. J. Mallorga, D.M. Pascarella, M.A. Snyder, J.B. Williams, Z. Zeng, The effects of deleting the mouse neurotensin receptor NTR1 on central and peripheral responses to neurotensin, J. Pharmacol. Exp. Ther. 300 (1) (2002) 305–313.
[97] B.M. Tyler, K. Jansen, D.J. McCormick, C.L. Douglas, M. Boules, J.A. Stewart, L. Zhao, B. Lacy, B. Cusack, A. Fauq, E. Richelson, Peptide nucleic acids targeted to the neurotensin receptor and administered i.p. cross the blood-brain barrier and specifically reduce gene expression, Proc. Natl. Acad. Sci. USA 96 (12) (1999) 7053–7058.
[98] J.A. Mechanic, J.E. Sutton, A.E. Berson, X. Wu, J. Kwan, R. Schreiber, Z. Pang, D. C. Button, Involvement of the neurotensin receptor 1 in the behavioral effects of two neurotensin agonists, NT-2 and NT69L: lack of hypothermic, antinociceptive and antipsychotic actions in receptor knockout mice, Eur. Neuropsychopharmacol. 19 (7) (2009) 466–475.
[99] F. Mule, R. Serio, A. Postorino, T. Vetri, F. Bonvissuto, Antagonism by SR 48692 of mechanical responses to neurotensin in rat intestine, Br. J. Pharm. 117 (3) (1996) 488–492.

[100] R. Carraway, S.E. Leeman, The isolation of a new hypotensive peptide, neurotensin, from bovine hypothalami, J. Biol. Chem. 248 (19) (1973) 6854–6861.
[101] R. Kérouac, F. Rioux, S. St-Pierre, Mechanism of neurotensin-induced pressor effect and tachycardia in guinea pigs, Life Sci. 28 (22) (1981) 2477–2487.
[102] F. Rioux, R. Quirion, S. St-Pierre, D. Regoli, F.B. Jolicoeur, F. Belanger, A. Barbeau, The hypotensive effect of centrally administered neurotensin in rats, Eur. J. Pharm. 69 (3) (1981) 241–247.
[103] M. Oishi, C. Inagaki, M. Fujiwara, S. Takaori, H. Yajima, Y. Akazawa, Possible mechanisms of the triphasic effects of neurotensin on the rat blood pressure, Jpn J. Pharm. 31 (6) (1981) 1043–1049.
[104] P. Kitabgi, P. Freychet, Effects of neurotensin on isolated intestinal smooth muscles, Eur. J. Pharm. 50 (4) (1978) 349–357.
[105] H.D. Allescher, H. Fick, V. Schusdziarra, M. Classen, Mechanisms of neurotensin-induced inhibition in rat ileal smooth muscle, Am. J. Physiol. 263 (5 Pt 1) (1992) G767–G774.
[106] N. Aronin, R.E. Carraway, C.F. Ferris, R.A. Hammer, S.E. Leeman, The stability and metabolism of intravenously administered neurotensin in the rat, Peptides 3 (4) (1982) 637–642.
[107] F. Checler, J.P. Vincent, P. Kitabgi, Degradation of neurotensin by rat brain synaptic membranes: involvement of a thermolysin-like metalloendopeptidase (enkephalinase), angiotensin-converting enzyme, and other unidentified peptidases, J. Neurochem. 41 (2) (1983) 375–384.
[108] F. Checler, P.C. Emson, J.P. Vincent, P. Kitabgi, Inactivation of neurotensin by rat brain synaptic membranes. Cleavage at the Pro10-Tyr11 bond by endopeptidase 24.11 (enkephalinase) and a peptidase different from proline-endopeptidase, J. Neurochem. 43 (5) (1984) 1295–1301.
[109] F. Checler, J.P. Vincent, P. Kitabgi, Inactivation of neurotensin by rat brain synaptic membranes partly occurs through cleavage at the Arg8-Arg9 peptide bond by a metalloendopeptidase, J. Neurochem. 45 (5) (1985) 1509–1513.
[110] F. Checler, J.P. Vincent, P. Kitabgi, Purification and characterization of a novel neurotensin-degrading peptidase from rat brain synaptic membranes, J. Biol. Chem. 261 (24) (1986) 11274–11281.
[111] J.D.A. Tyndall, T. Nall, D.P. Fairlie, Proteases universally recognize beta strands in their active sites, Chem. Rev. 105 (3) (2005) 973–999.
[112] A. Taneja, O. Della Pasqua, M. Danhof, Challenges in translational drug research in neuropathic and inflammatory pain: the prerequisites for a new paradigm, Eur. J. Clin. Pharm. 73 (10) (2017) 1219–1236.
[113] I. Tracey, C.J. Woolf, N.A. Andrews, Composite pain biomarker signatures for objective assessment and effective treatment, Neuron 101 (5) (2019) 783–800.
[114] J.F. Gainor, D.L. Longo, B.A. Chabner, Pharmacodynamic biomarkers: falling short of the mark? Clin. Cancer Res. 20 (10) (2014) 2587–2594.
[115] K.D. Davis, N. Aghaeepour, A.H. Ahn, M.S. Angst, D. Borsook, A. Brenton, M. E. Burczynski, C. Crean, R. Edwards, B. Gaudilliere, G.W. Hergenroeder, M. J. Iadarola, S. Iyengar, Y. Jiang, J.T. Kong, S. Mackey, C.Y. Saab, C.N. Sang, J. Scholz, M. Segerdahl, I. Tracey, C. Veasley, J. Wang, T.D. Wager, A.D. Wasan, M.A. Pelleymounter, Discovery and validation of biomarkers to aid the development of safe and effective pain therapeutics: challenges and opportunities, Nat. Rev. Neurol. 16 (7) (2020) 381–400.